iScience

CellPress
OPEN ACCESS

Article

Differential Regulation of mTOR Complexes with miR-302a Attenuates Myocardial Reperfusion Injury in Diabetes

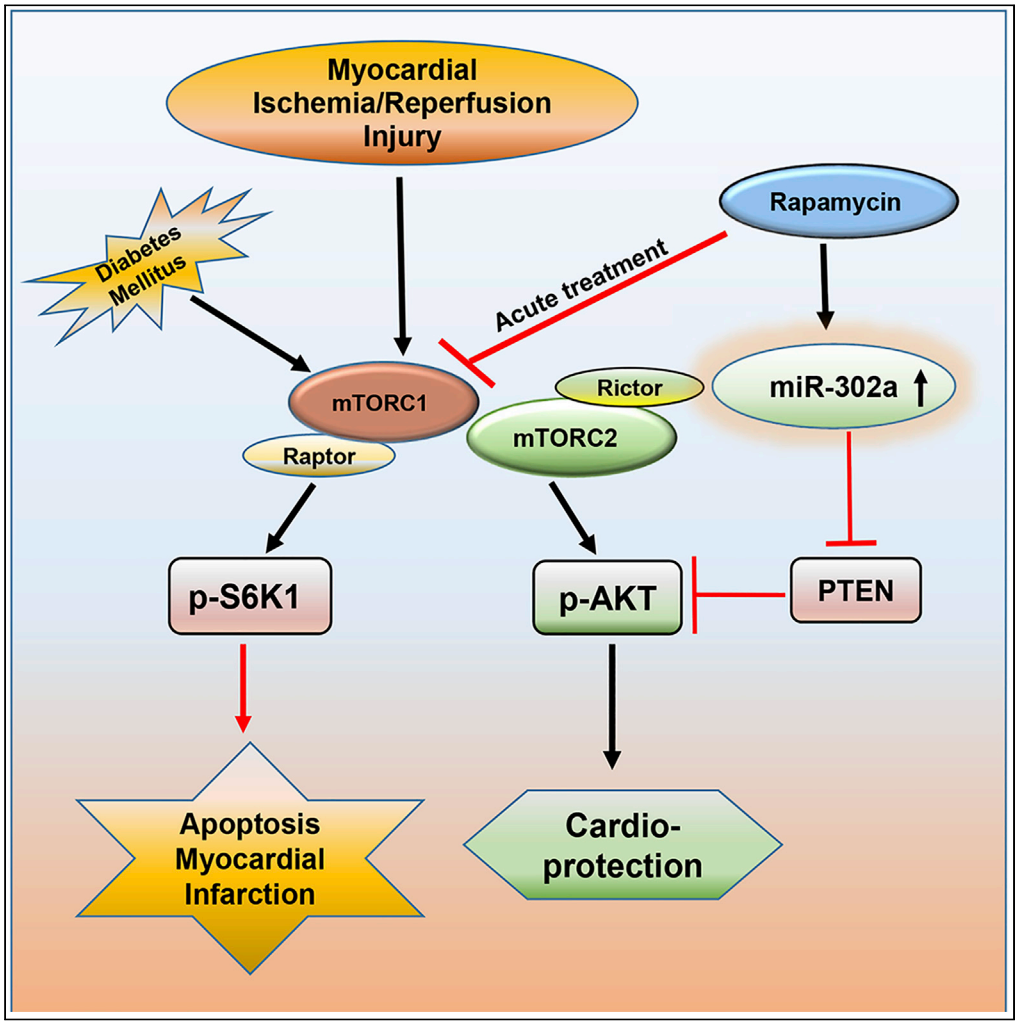

Arun Samidurai, Ramzi Ockaili, Chad Cain, ..., Donatas Kraskauskas, Rakesh C. Kukreja, Anindita Das

rakesh.kukreja@vcuhealth.org (R.C.K.)
anindita.das@vcuhealth.org (A.D.)

HIGHLIGHTS

miR-302a and AKT phosphorylation are suppressed in post-ischemic diabetic heart

Negative regulator of insulin signaling, PTEN, is induced after ischemia reperfusion

miRNA-302a-mimic abolishes ischemic injury in hyperglycemic human iPS cardiocytes

Rapamycin treatment restores miR-302a-mTORC2 cardioprotective signaling in diabetes

Samidurai et al., iScience *23*, 101863
December 18, 2020 © 2020
https://doi.org/10.1016/j.isci.2020.101863

iScience

CellPress
OPEN ACCESS

Article

Differential Regulation of mTOR Complexes with miR-302a Attenuates Myocardial Reperfusion Injury in Diabetes

Arun Samidurai,[1] Ramzi Ockaili,[1] Chad Cain,[1] Sean K. Roh,[1] Scott M. Filippone,[1] Donatas Kraskauskas,[1] Rakesh C. Kukreja,[1,*] and Anindita Das[1,2,*]

SUMMARY

Persistent activation of mTOR (mammalian target of rapamycin) in diabetes increases the vulnerability of the heart to ischemia/reperfusion (I/R) injury. We show here that infusion of rapamycin (mTOR inhibitor) at reperfusion following ischemia reduced myocardial infarct size and apoptosis with restoration of cardiac function in type 1 diabetic rabbits. Likewise, treatment with rapamycin protected hyperglycemic human-pluripotent-stem-cells-derived cardiomyocytes (HG-hiPSC-CMs) following simulated ischemia (SI) and reoxygenation (RO). Phosphorylation of S6 (mTORC1 marker) was increased, whereas AKT phosphorylation (mTORC2 marker) and microRNA-302a were reduced with concomitant increase of its target, PTEN, following I/R injury in diabetic heart and HG-hiPSC-CMs. Rapamycin inhibited mTORC1 and PTEN, but augmented mTORC2 with restoration of miRNA-302a under diabetic conditions. Inhibition of miRNA-302a blocked mTORC2 and abolished rapamycin-induced protection against SI/RO injury in HG-hiPSC-CMs. We conclude that rapamycin attenuates reperfusion injury in diabetic heart through inhibition of PTEN and mTORC1 with restoration of miR-302a-mTORC2 signaling.

INTRODUCTION

Diabetes mellitus (DM) is one of the major risk factors for developing coronary heart disease (Hinkel et al., 2017). Despite recent progress in coronary intervention strategies, diabetic patients are potentially susceptible to myocardial ischemia/reperfusion (I/R) injury, which is associated with higher mortality rate after the incidence of acute myocardial infarction (AMI) (Ding et al., 2017; Miki et al., 2012). Diabetes mellitus (DM) also influences myocardial responses to conditioning stimuli (pre- and post-conditioning) by disrupting the intracellular signaling responsible for cardioprotection (Lejay et al., 2016; Miki et al., 2012). Population-based studies estimate that 14%–45% of children as well as youth with type 1 diabetes (T1D) have increased risk for premature morbidity and mortality due to cardiovascular diseases (de Ferranti et al., 2014; Margeirsdottir et al., 2008). The annual incidence of T1D among youths showed significant linear increase worldwide during the year of 2002–2012 (Mayer-Davis et al., 2017). Hyperglycemia stimulates the production of advanced glycation end products (AGE), accumulation of free radicals, polyol, and hexosamine flux with an increase in intravascular inflammatory response as well as oxidizes low-density lipoproteins (LDL), which promote vascular damage and accelerate the atherosclerotic progression and microvascular dysfunction (Severino et al., 2019; Sima et al., 2010). These mechanisms are the basis of myocardial ischemia as well as chronic kidney injury, retinopathy, and the most important complications associated with DM (Jha et al., 2018; Ungurianu et al., 2017). ApoE (apolipoprotein E)-null mice treated with streptozotocin (STZ) to induce T1D developed enhanced atherosclerosis with an increased plasma level of AGEs compared with euglycemic ApoE-null mice (Park et al., 1998). Further studies in cardiomyocytes from the AGE receptor (RAGE)-knockout mice confirmed that the genetic deletion and pharmacological blockade of RAGE alleviate cellular injury in cardiomyocytes upon hypoxia/reoxygenation through JNK/GSK-3β signaling pathway (Shang et al., 2010).

The mammalian target of rapamycin (mTOR) pathway governs numerous cellular signaling involved in cell growth, proliferation, cellular metabolism, ribosomal biogenesis, protein translation as well as cell death

[1]Division of Cardiology, Pauley Heart Center, Box 980204, Virginia Commonwealth University Medical Center, 1101 East Marshall Street, Sanger Hall, Room 7020d & 7020b, Richmond, VA 23298-0204, USA

[2]Lead Contact

*Correspondence: rakesh.kukreja@vcuhealth.org (R.C.K.), anindita.das@vcuhealth.org (A.D.)

https://doi.org/10.1016/j.isci.2020.101863

including apoptosis, autophagy, and necroptosis (Loewith et al., 2002; Thoreen et al., 2012). The mTOR plays a central role in the maintenance and integration of cellular energy status and oxygen level (Arsham et al., 2003) and functions as stress indicator in response to stimuli, such as insulin, insulin growth factor, and glucose (Chung et al., 1994; Dennis et al., 2001). The mTOR, a serine/threonine protein kinase, exists in two complex forms, mTORC1 and mTORC2. These two complexes not only share some common components, but also contain unique subunits (Laplante and Sabatini, 2012). The mTORC1 is inhibited by rapamycin (RAPA), whereas mTORC2 is significantly less sensitive to RAPA, only inhibited by chronic treatment in certain cell types and tissues (Sarbassov et al., 2006). Hyperglycemia leads to robust activation of mTOR with worsening of diabetic complications including the myocardial I/R injury (Das et al., 2015; Stamateris et al., 2016). Activation of mTORC2-AKT (Protein kinase B) signaling plays a pivotal role in cardioprotection against I/R injury (Volkers et al., 2013; Yano et al., 2014). We previously demonstrated that mTOR is persistently activated in the hearts of diabetic mice (Das et al., 2014) and chronic pre-treatment with RAPA improved cardiac function and reduced infarct size following I/R injury (Das et al., 2014; Samidurai et al., 2017, 2019). In addition, RAPA-treatment protects myocardial reperfusion injury in diabetic mice through STAT3-mTORC2 signaling (Das et al., 2015). However, the underlying molecular mechanism that triggers mTORC2 activation in diabetic heart following RAPA treatment is currently unknown.

The tumor suppressor phosphatase and tensin homologue (PTEN) is a major homeostatic regulator, by virtue of its lipid phosphatase activity against phosphatidylinositol 3,4,5-trisphosphate [PI(3,4,5)P3] (Pulido, 2018). PTEN negatively regulates AKT in ischemic heart (Parajuli et al., 2012), whose activity is modulated by its abundance, oxidation, or phosphorylation (Leslie et al., 2008). PTEN has been regarded as the Achilles' heel of the myocardium, because its knockdown reduces infarction following MI (Ruan et al., 2009). Pharmacological inhibition of PTEN enhances PI3K activity and attenuates myocardial I/R injury (Keyes et al., 2010). Cardiac-specific PTEN inactivation prevents maladaptive ventricular remodeling with preservation of angiogenesis following pressure overload in mice (Oudit et al., 2008). Also, myocyte-specific PTEN deficiency attenuates post-MI remodeling by increasing AKT phosphorylation (Parajuli et al., 2012).

MicroRNAs (miRs), the small non-coding RNAs (~25 nucleotide length), have emerged as the critical regulators of various cardiac physiological and pathological processes, including organ development, arrhythmias, hypertrophy, fibrosis, apoptosis, vessel remodeling, and angiogenesis (Wang et al., 2010). Different miRs, which regulate PTEN in many pathophysiological cardiac processes (Glass and Singla, 2011; Ling et al., 2013; Sayed et al., 2010), have been identified as the potential therapeutic targets for cardioprotection. A previous study showed that overexpression of miR-302a improved cardiac regeneration, increased cardiomyocyte proliferation and survival with improved vessel formation in the peri-infarct region, and decreased fibrosis (Tian et al., 2015). miR-302a reduces neurotoxicity by activating AKT through silencing PTEN, which restores the insulin signaling in patients with diabetes-induced neurodegenerative diseases (Li et al., 2016). We hypothesize that treatment with RAPA at the onset of reperfusion would reduce myocardial infarct size following ischemia in diabetic rabbits by inhibiting mTORC1, while restoring mTORC2. We further contemplated that the increased expression of miR-302a may inhibit PTEN, with consequent increase of mTORC2 activity indicated by phosphorylation of AKT (Ser^{473}) in the diabetic hearts as well as human-induced pluripotent-stem-cells-derived cardiomyocytes (hiPSC-CMs) following reperfusion injury.

RESULTS

Induction of Type 1 Diabetes

Four weeks after alloxan treatment (125 mg/kg, i.v.), 57 out of 63 rabbits survived and 53 rabbits had blood glucose level greater than 220 mg/dL, which were considered as diabetic. The average glucose level was 342.2 $\pm$ 11.2 mg/dL as indicated by red line (Figure 1A). The success rate of induction of diabetes was 84.1% with 9.5% mortality after alloxan treatment.

Rapamycin Administration at Reperfusion Limits Infarct Size

Figure 1B shows experimental protocol in the rabbit model of conscious MI, administration of RAPA at the onset of reperfusion, the time points for blood collection, measurement of infarct size, apoptosis, and protein expression. Table S1 (supplement) shows the body weight, age, blood glucose, and heart weight of control and diabetic rabbits with/without RAPA treatment, measured at the end of the protocol. Body weight and age were comparable among assigned cohorts. Blood glucose levels were significantly higher in DM, DM + I/R, and DM + I/R + RAPA groups as compared with control and I/R. Within 72 h of reperfusion, 5 out of 23 diabetic rabbits died in DM + I/R group, whereas animals in DM + I/R + RAPA cohort had no

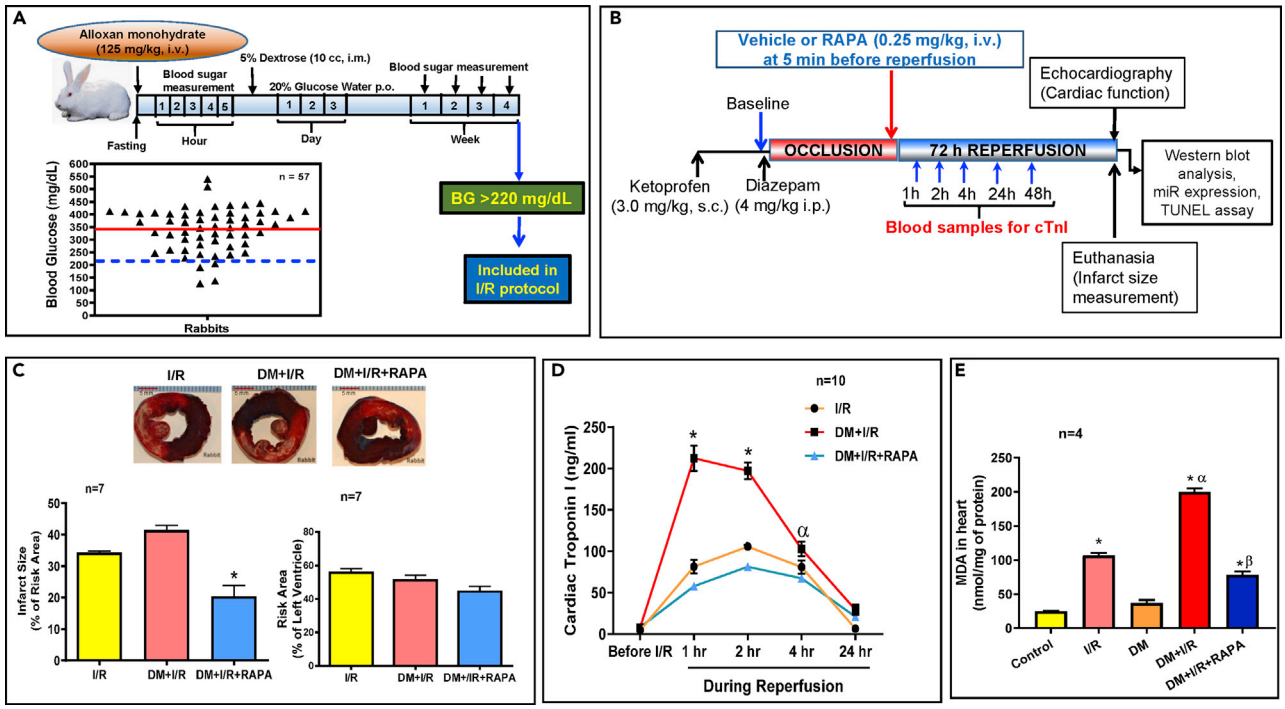

Figure 1. Infarct Limiting Effect of Rapamycin (RAPA) in Diabetic Rabbits Following Ischemia/Reperfusion (I/R) Injury

(A) Experimental protocol for inducing T1D. Rabbits were treated with alloxan monohydrate and blood glucose levels were monitored for 4 weeks. Animals with consistent blood sugar of 220 mg/dL (blue dashed line) or above were considered diabetic. The average blood glucose level is denoted by red line.

(B) Experimental Protocol for I/R in conscious diabetic rabbits.

(C) Myocardial infarct size (% of risk area) and risk area (% of LV). Scale indicates 5 mm. n = 7/group; *p < 0.001 versus I/R and DM + I/R.

(D) Plasma levels of cardiac troponin I following I/R in controls (I/R), diabetics rabbits (DM + I/R), and diabetic rabbit treated with RAPA at the onset of reperfusion (DM + I/R + RAPA). n = 10; *p < 0.0001 versus I/R and DM + I/R + RAPA; $^{\alpha}$p<0.01 versus DM + I/R + RAPA.

(E) Oxidative stress was measured by lipid peroxidation assay for formation of malondialdehyde (MDA) in the hearts. n = 4; *p < 0.0001 versus control and DM; $^{\alpha}$p<0.0001 versus I/R; $^{\beta}$p<0.0001 versus DM + I/R. Statistics: one-way ANOVA. Data are represented as mean ± SEM.

mortality. Figure 1C shows that infarct size in the diabetics was higher as compared with the non-diabetic rabbits (although non-significant, p > 0.08). Treatment with RAPA reduced infarct size as compared with the non-diabetic as well as diabetic groups. The risk area was not statistically different between the groups. Post I/R plasma cardiac troponin I (cTnI) levels significantly increased at 1, 2, and 4 h of reperfusion, which were more prominent in diabetic animals (Figure 1D). Treatment with RAPA reduced cTnI release following I/R injury. The oxidative stress was significantly increased following I/R both in the non-diabetic and diabetic hearts (Figure 1E). RAPA treatment significantly attenuated post-I/R MDA accumulation in diabetic hearts, suggesting a potent antioxidant effect of RAPA.

Rapamycin Restores Post-ischemic Cardiac Function

All groups displayed a normal and comparable left ventricular (LV)-systolic function prior to the induction of diabetes and MI. After 4 weeks of alloxan treatment, LV ejection fraction (LVEF) was not affected in diabetic rabbits as compared with control prior to I/R injury (Figure 2). A statistically significant decline in LVEF was observed in the control and DM groups at 72h post-MI. Treatment with RAPA significantly restored LVEF in post-MI diabetic rabbits. There were no significant differences of LV-end-systolic diameter (LVESD), LV-end-diastolic diameter (LVEDD), cardiac output (CO), stroke volume (SV), and heart rate (HR) between groups (Figure S1).

Rapamycin Treatment has No Adverse Effect on Hemodynamics

Hemodynamics were recorded at baseline, 1 and 2 h after occlusion in control and diabetic rabbit with/without RAPA treatment (Figure S2). There was no significant difference in the mean arterial pressure, systolic pressure, and diastolic pressure and heart rate between control, DM + I/R, and DM + I/R + RAPA groups. These results suggest that RAPA treatment at reperfusion had no adverse effect on the hemodynamics. In addition, the heart rate was stable during the I/R protocol.

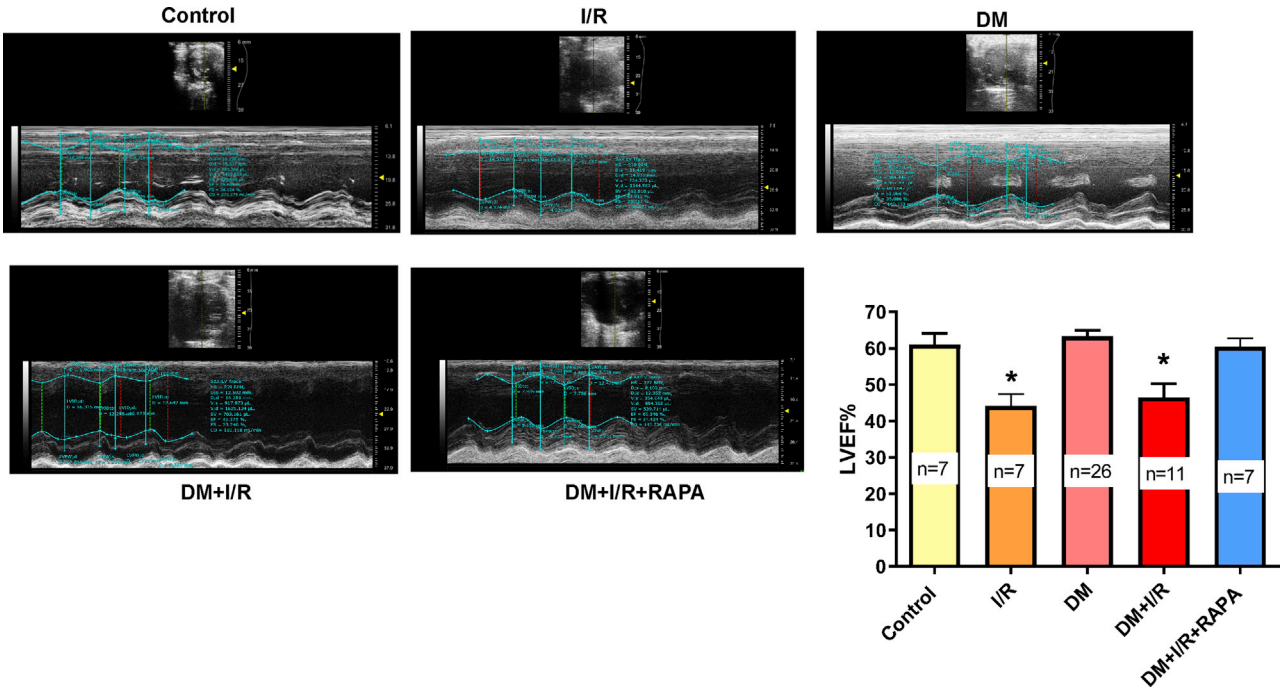

Figure 2. Rapamycin (RAPA) Restores Post-Ischemic Cardiac Function in Diabetic Rabbits

Representative images of parasternal long-axis view (M-mode ultrasound) assessing LVEF at baseline indicates the cardiac function of control rabbits before/without I/R. I/R indicates LVEF after 45 min I and 72 hours of reperfusion in control rabbits. Diabetic rabbits were treated with RAPA at the onset of reperfusion (DM + I/R + RAPA). *p < 0.05 versus control, DM, and DM + I/R + RAPA. Statistics: one-way ANOVA. Data are represented as mean ± SEM.

Rapamycin Attenuates Cardiac Apoptosis

There was significant increase in TUNEL-positive nuclei in the peri-infarct regions in the diabetic hearts following I/R as compared with the non-diabetic hearts (Figures 3A and 3B). Reperfusion with RAPA reduced apoptotic nuclei by 33% in diabetic hearts. Bcl-2 expression was not altered following I/R, although Bax was significantly increased in both control and diabetic rabbit hearts (Figure 3C). RAPA significantly induced Bcl-2 expression in the diabetic heart, without altering Bax. In totality, the Bcl-2 to Bax ratio was significantly reduced in I/R and DM + I/R groups, but it was restored in the DM + I/R + RAPA group compared with others.

Differential Activation of mTOR Complexes during Ischemia/Reperfusion

To investigate the underlying mechanism of the anti-ischemic effect of RAPA, we examined the markers of mTORC1 and C2 by measuring the phosphorylation of ribosomal S6 ($Ser^{235/236}$) and AKT (Ser^{473}), respectively. There was no significant difference in the level of S6 phosphorylation in the control and diabetic hearts (Figure 4A). After I/R injury, S6 phosphorylation increased in the control and diabetic hearts, suggesting mTORC1 activation. Notably, post-I/R induction of S6 phosphorylation was more pronounced in diabetic heart, which was abolished following RAPA treatment, suggesting specific inhibition of mTORC1. The total S6 in relation to GAPDH (glyceraldehyde 3-phosphate dehydrogenase) was increased in RAPA-treated diabetic heart following I/R injury. Concurrently, phosphorylation of AKT (Ser^{473}) was decreased in the control and diabetic hearts following I/R injury, suggesting inactivation of mTORC2. The reduction of post-I/R phosphorylation of AKT (Ser^{473}) was more distinct in diabetic hearts. Treatment with RAPA activated mTORC2 as demonstrated by restoration of post-I/R phosphorylation of AKT (Ser^{473}) as well as total AKT in the diabetic hearts. However, phosphorylation of AKT at Thr 308 did not change between groups (Figure S3).

Rapamycin Increases miRNA-302a and Regulates PTEN

Based on miRBase database for rabbit-specific miRNAs, within twelve annotated miRNAs (Table S2A), we examined the expression of nine different miRNAs in control and diabetic rabbit heart before/after I/R and with/without RAPA treatment (Figures 4B and S4). The real-time PCR data revealed a significant reduction

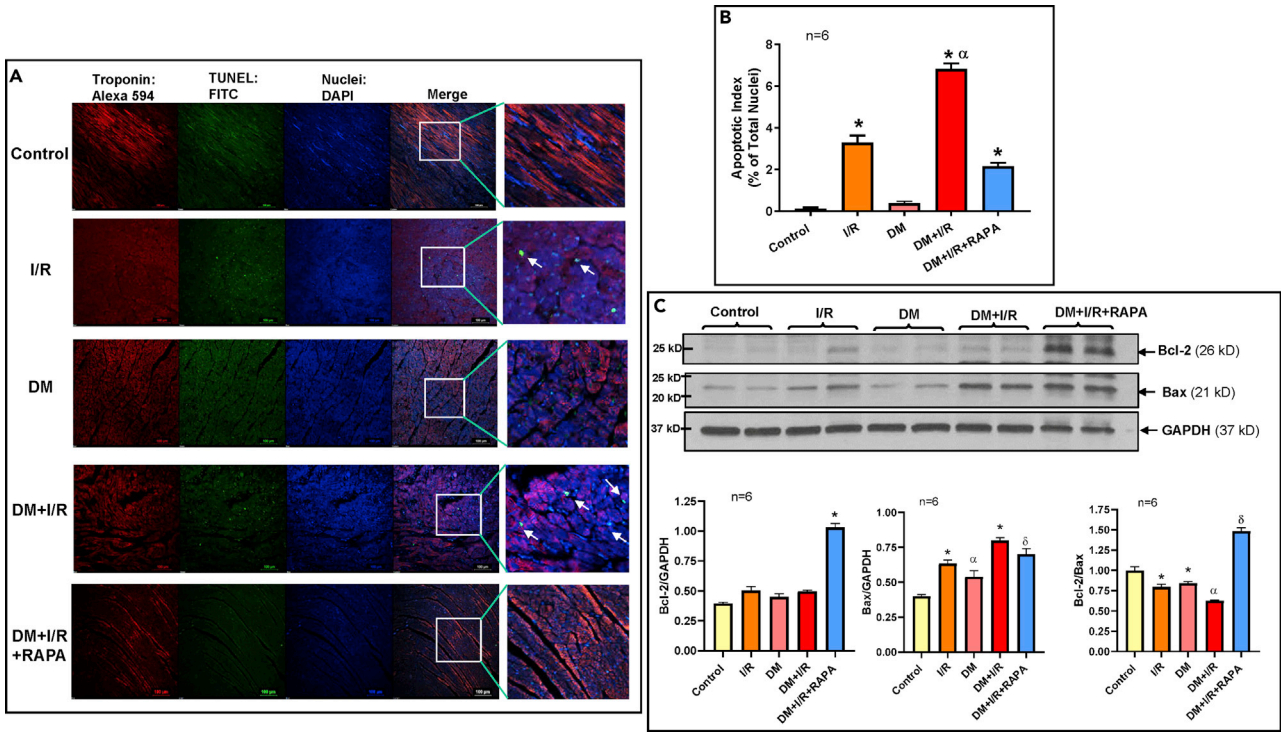

Figure 3. Rapamycin (RAPA) Reduces Myocardial Apoptosis Following I/R Injury in Diabetic Rabbits

(A) Apoptosis in the LV risk area was assessed by TUNEL assay. Representative pictures of TUNEL (Green), DAPI (Blue), and troponin (Red: Alexa 594) staining. Scale indicates 100 μm.

(B) Percentage of apoptotic nuclei to total nuclei in control, I/R, DM, DM + I/R, and DM + IR + RAPA groups. n = 6; *p < 0.0001 versus control and DM; $^{\alpha}$p<0.0001 versus others.

(C) Representative immunoblots showing expression of Bcl-2 and Bax and densitometry analysis of the ratio of Bcl-2 to GAPDH (n = 6; *p < 0.0001 versus others); Bax to GAPDH (n = 6; *p < 0.0001 versus control and DM; $^{\alpha}$p<0.0001 versus control; $^{\delta}$p<0.01 versus control and DM); Bcl-2 to Bax (n = 6; *p < 0.05 versus control; $^{\alpha}$p<0.01 versus control, I/R and DM; $^{\delta}$p<0.0001 versus others). Statistics: one-way ANOVA. Data are represented as mean ± SEM.

of miR-302a among all the analyzed miRs in the control hearts following I/R injury (Figure 4B), which reduced even more in the diabetic heart. Treatment with RAPA restored the expression of miR-302a. Based on the bioinformatics evidence (www.targetscan.org), we identified PTEN as a potential target of miR-302a (Figure S5A), which was confirmed by real-time PCR with significant increase in the PTEN mRNA following I/R in both control and even more distinctly in the diabetic hearts (Figure 4C). RAPA treatment reduced PTEN mRNA level following I/R in diabetic heart, suggesting inverse relationship with miR-302a. Likewise, the expression of PTEN protein was increased in the diabetic heart following I/R injury (Figure 4D), which was attenuated by treatment with RAPA.

miR-302a Directly Regulates PTEN-AKT in Human Cardiomyocytes

To further interrogate the cause and effect relationship of miR-302a in regulating PTEN-AKT signaling and to demonstrate the human relevance of these findings, we used spontaneously beating hiPSC-CMs, which were exposed to either normal glucose (NG) or high D-glucose (HG) conditions. The necrosis and apoptosis were significantly increased following simulated ischemia/reoxygenation (SI/RO) under NG condition (Figures 5A–5C), which was further augmented under HG condition. RAPA treatment at RO significantly protected hiPSC-CMs against SI/RO injury by reducing necrosis and apoptosis under both NG and HG conditions. However, there was no significant effect of 25 mM L-glucose (the inactive enantiomer) on necrosis of hiPSC-CMs as compared with NG before and after SI/RO (Figure S6A), ruling out any potential non-specific osmotic effect of HG.

The miR-302a level was reduced in hiPSC-CMs following SI/RO injury under NG as well as HG conditions (Figure 5D), which was restored by RAPA treatment under both conditions. In consistence with these results, the PTEN mRNA increased after SI/RO in hiPSC-CMs, which further increased under HG conditions

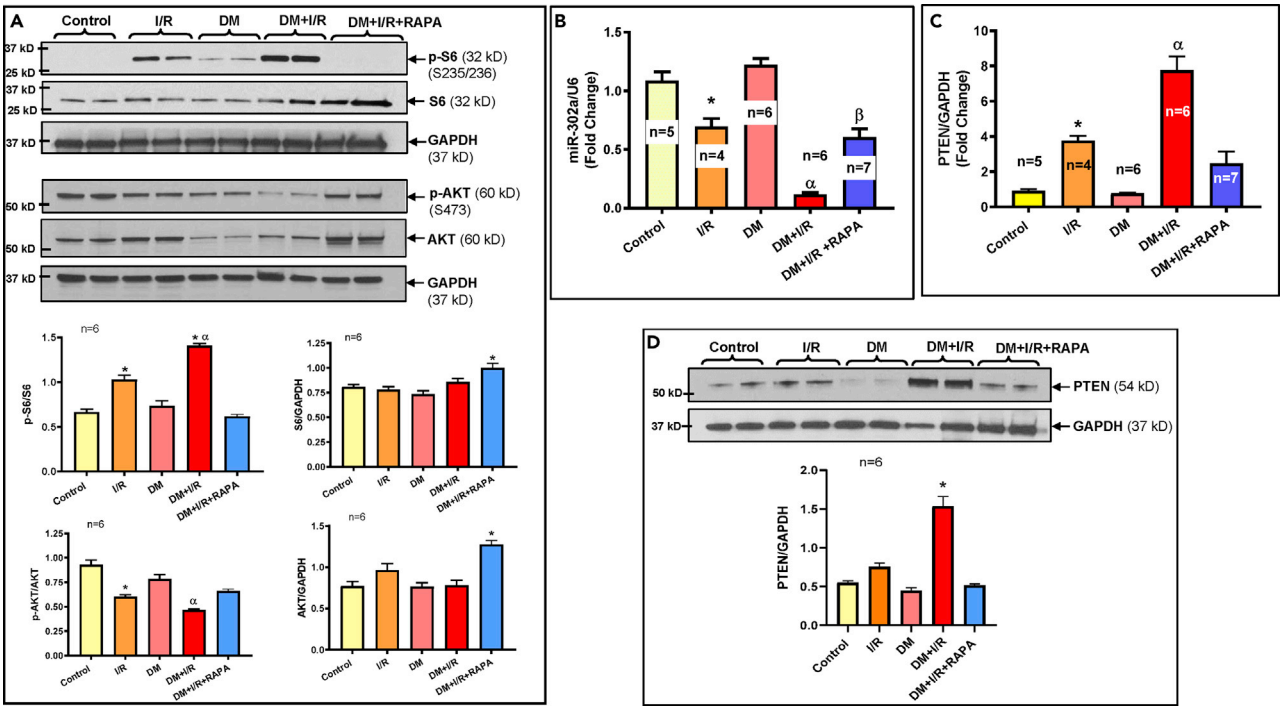

Figure 4. Rapamycin Differentially Regulates mTORC1 and mTORC2 in Diabetic Rabbits Following I/R Injury

(A) Upper panel shows the representative immunoblots and lower panel shows densitometry analysis of the ratios of phosphorylation of S6 to total S6 (p-S6/S6; n = 6; *p < 0.0001 versus control, DM, DM + I/R + RAPA; $^{\alpha}$p<0.0001 versus I/R), phosphorylation of AKT to total AKT (p-AKT/AKT; n = 6; *p < 0.01 versus control and DM; $^{\alpha}$p<0.0001 versus control, DM and DM + I/R + RAPA), and total proteins to GAPDH (S6/GAPDH; n = 6; *p < 0.05 versus control, I/R and DM and AKT/GAPDH; n = 6; *p < 0.001 versus others).

(B) Real-time PCR analysis shows the levels of miR-302a (*p < 0.05 versus control and DM; $^{\alpha}$p<0.001 versus others and $^{\beta}$p<0.001 versus control and DM).

(C) Real-time PCR analysis shows the levels of PTEN mRNA (*p < 0.05 versus control and DM; $^{\alpha}$p<0.001 versus others).

(D) Representative immunoblots (upper panel) and densitometry analysis (lower panel) of the expression of PTEN and GAPDH in hearts of control and diabetic rabbits before/after I/R and with/without RAPA treatment (n = 6; *p < 0.0001 versus others). Statistics: one-way ANOVA. Data are represented as mean ± SEM.

(Figure 5E). Likewise, PTEN mRNA was normalized following RAPA treatment under NG/HG conditions following SI/RO.

To further demonstrate the direct role of - miR-303a in RAPA-induced protection against SI/RO under NG/HG conditions, we used an LNA-based specific inhibitor to block the binding of miR-302a to PTEN mRNA. The results showed that miR-302a inhibitor abolished the protective effect of RAPA against SI/RO under NG/HG conditions in hiPSC-CMs as shown by increased necrosis (Figure 6A), attenuation of Bcl-2, and increase in Bax expression (Figure 6B). The activation of mTORC1 following SI/RO injury was increased as indicated by S6 phosphorylation under NG conditions, which was increased much higher under HG condition (Figure 6C). Treatment with RAPA completely blocked S6 phosphorylation following SI/RO injury under both NG and HG conditions. Similar to the diabetic heart, SI/RO reduced AKT phosphorylation (Ser^{473}) in hiPSC-CMs, and RAPA restored AKT phosphorylation under both NG and HG conditions, suggesting mTORC2 activation. RAPA-induced AKT phosphorylation (Ser^{473}) following SI/RO injury was obliterated with the inhibitor of miR-302a. Conversely, miR-302a inhibitor had no effect on S6 phosphorylation (Figure 6C).

Treatment with RAPA also attenuated post-SI/RO induction of PTEN in hiPSC-CMs under both NG and HG conditions (Figure 6D), which was completely reversed by miR-302a inhibitor. Moreover, the results showed interaction between miR-302a and PTEN mRNA, which was confirmed by direct binding of miR-302a to the 3'UTR of PTEN mRNA in the dual luciferase reporter assay (Figure S5B).

To further elucidate the protective role of miR-302a against SI/RO injury, we utilized hsa-miR-302a-3p mimic (miR-302a mimic) in hiPSC-CMs (Figure S6B). The results showed reduced necrosis and apoptosis following

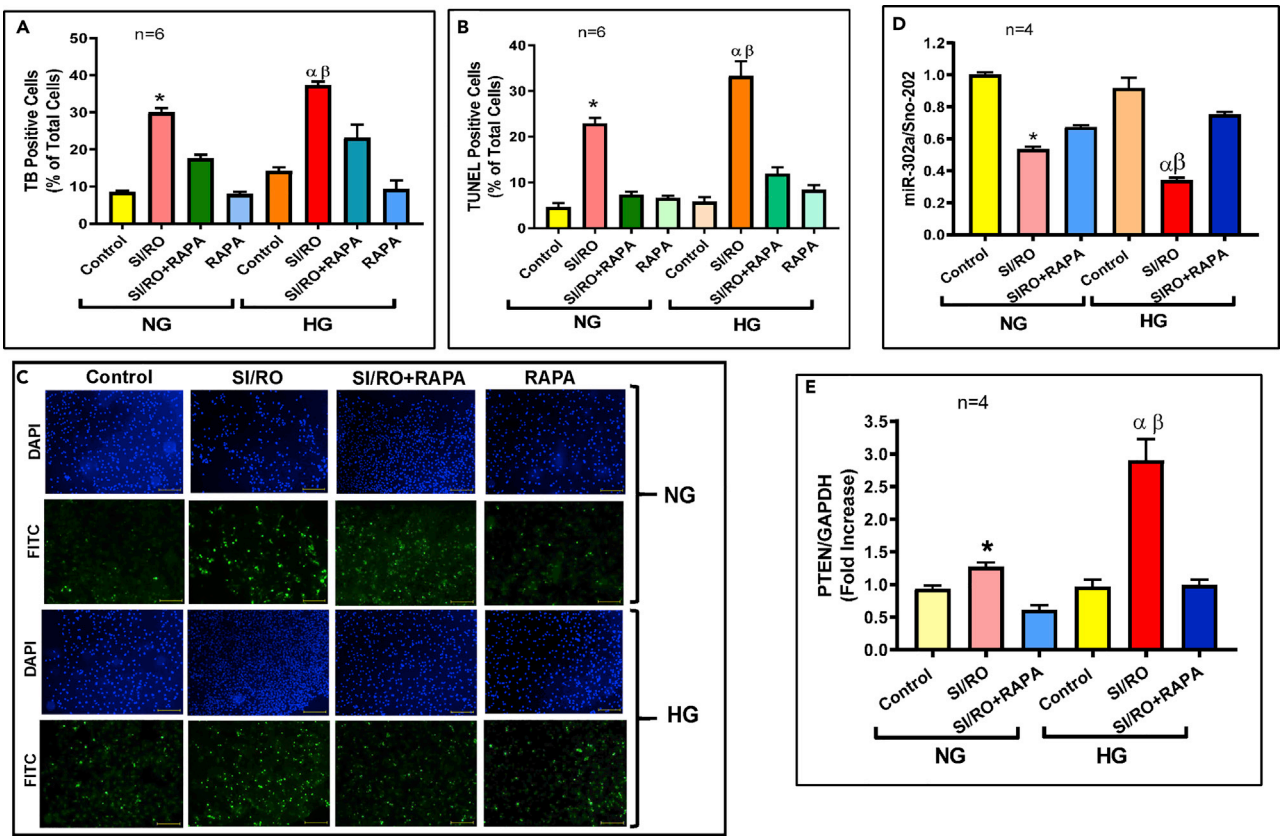

Figure 5. Rapamycin (RAPA) Protects hiPSC-CM Cells Against Simulated Ischemia and Reoxygenation (SI/RO) Injury Under Normal (NG) and High Glucose (HG) Conditions: Role of miR-302a and PTEN.

(A) hiPSC-CM necrosis (n = 6; *p < 0.0001 versus others (NG); $^{\alpha}$p<0.0001 versus others (HG); $^{\beta}$p<0.001 versus SI/RO (NG)).

(B) hiPSC-CM apoptosis (n = 6; *p < 0.005 versus others (NG); $^{\alpha}$p<0.0001 versus others (HG); $^{\beta}$p<0.05 versus SI/RO (NG)).

(C) Representative pictures of TUNEL-DAPI staining of hiPSC-CMs following SI/RO under NG and HG. Scale indicates 100 μm.

(D Real-time PCR quantitation of miR-302a following SI/RO injury with/without RAPA (100 nM; during RO). Sno-202 was used to normalize miR-302a expression. n = 4; *p < 0.05 versus control (NG) and SI/RO + RAPA (NG); $^{\alpha}$p<0.0001 versus control (HG) and SI/RO + RAPA (HG); $^{\beta}$p<0.0001 versus SI/RO (NG).

(E) Real-time PCR analysis of PTEN mRNA under identical conditions as described under (D). GAPDH was used to normalize PTEN levels. (n = 4; *p < 0.05 versus control (NG) and SI/RO + RAPA (NG); $^{\alpha}$p<0.001 versus control (HG) and SI/RO + RAPA (HG); $^{\beta}$p<0.001 versus SI/RO (NG). Statistics: one-way ANOVA. Data are represented as mean ± SEM.

SI/RO in hiPSC-CMs overexpressing miR-302a under both NG and HG conditions (Figures 7A and 7B) with associated restoration of Bcl-2 as well as Bcl-2/Bax ratio (Figure 7C). miR-302a mimic had no effect on the post-SI/RO activation of mTORC1 as indicated by enhanced S6 phosphorylation (Figure 8A), but it restored mTORC2 activity as indicated by increased phosphorylation of AKT (Ser^{473}) under both NG and HG conditions (Figure 8B). Moreover, miR-302a mimic suppressed the induction of PTEN following SI/RO in hiPSC-CMs under NG and HG conditions (Figure 8C). In summary, these results provide conclusive evidence that RAPA-induced protection against SI/RO in hiPSC-CMs is mediated by restoration of miR-302a level under both NG and HG conditions.

DISCUSSION

Salient Findings

Diabetes mellitus escalates myocardial susceptibility to I/R injury, which is associated with poor prognosis and eventually higher mortality following AMI. A large retrospective study of patients reported that post-conditioning (by intermittent episodes of ischemia)-induced cardioprotection against AMI was impaired in the diabetic cohort (Yetgin et al., 2014). The mechanisms contributing to the pathogenesis of exacerbated myocardial I/R injury associated with comorbid conditions, such as diabetes, are multifactorial, complex, and highly integrated. Currently there are no therapeutic strategies to reduce I/R injury in the diabetic heart. In the present study, we investigated the effect of mTOR inhibitor, RAPA, in protecting against

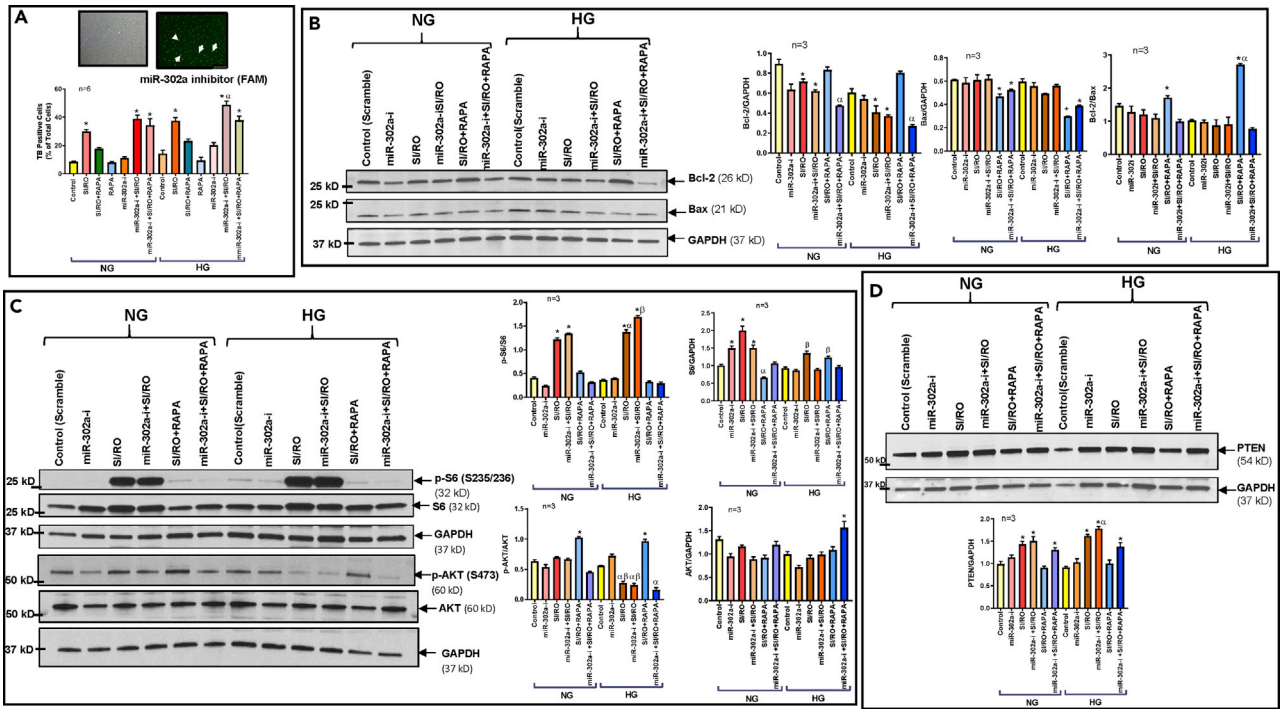

Figure 6. miR-302a Inhibition in hiPSC-CMs Blocks Rapamycin (RAPA)-Induced Protection Against Simulated Ischemia and Reoxygenation (SI/RO) Injury Under Normal (NG) and High Glucose (HG) Conditions

(A) Representative picture (upper panel) showing transfection efficiency of miR-302a inhibitor (LNA)-labeled with FAM (Green) dye of hiPSC-CMs and necrosis of following SI/RO.n = 6; *p < 0.0001 versus control, SI/RO + RAPA, RAPA, miR-302a-i (NG/HG); $^{\alpha}$p<0.05 versus SI/RO (HG) and miR-302a-i + SI/RO (NG).

(B) Representative immunoblots showing the effect of miR-302a inhibitor on expression of Bcl-2 and Bax following SI/RO with or without RAPA (100 nM; during RO). Right panel shows the densitometry analysis of Bcl-2 to GAPDH (n = 3; *p < 0.01 versus control and SI/RO + RAPA; $^{\alpha}$p<0.001 versus SI/RO + RAPA); Bax to GAPDH (n = 3; *p < 0.01 versus control, SI/RO & 302a-i + SI/RO) and Bcl-2 to Bax ratio (n = 3; *p < 0.01 versus 302i + SI/RO; $^{\alpha}$p<0.001 versus SI/RO (HG)).

(C) Phosphorylation of S6 and AKT under NG and HG condition following SI/RO with or without RAPA (100 nM; during RO). Right panel: densitometry analysis of the ratios of p-S6/S6 (n = 3; *p < 0.0001 versus control, miR-302a-i, SI/RO + RAPA, and miR-302a-i + SI/RO + RAPA; $^{\alpha}$p<0.01 versus SI/RO (NG); $^{\beta}$p<0.001 versus SI/RO (HG)); S6/GAPDH (n = 3; *p < 0.001 versus control (NG) and SI/RO + RAPA (NG); $^{\alpha}$p<0.01 versus control (NG); $^{\beta}$p<0.05 versus control (HG) and miR-302a-i (HG)); p-AKT/AKT (n = 3; *p < 0.001 versus others; $^{\alpha}$p<0.05 versus control, miR-302a-i and SI/RO + RAPA (HG); $^{\beta}$p<0.0001 versus SI/RO (NG)); AKT/GAPDH (n = 3; *p < 0.01 versus others).

(D) PTEN expression under NG and HG conditions following SI/RO with or without RAPA treatment (100 nM; during RO). Lower panel shows densitometry analysis of PTEN with GAPDH as loading control. n = 3; *p < 0.01 versus control and SI/RO + RAPA; $^{\alpha}$p<0.05 versus miR-302a-i + SI/RO (NG). Statistics: one-way ANOVA. Data are represented as mean ± SEM.

myocardial reperfusion injury in a translational diabetic rabbit model of conscious MI and identified associated mechanisms of cardioprotection. Our results show that protective effect of RAPA in diabetic rabbits against reperfusion injury is associated with mTORC1 inhibition and simultaneous activation of mTORC2. In addition, treatment with RAPA at the onset of reperfusion induced miR-302a and inhibited its direct target PTEN, which coordinately restored AKT phosphorylation following I/R injury. Further studies in hiPSC-CMs revealed that inhibition of miR-302a abolished the protective effect of RAPA against SI/RO under HG condition by exerting negative impact on miR-302a-PTEN-AKT signaling pathway. However, the inhibition of mTORC1 with RAPA was insensitive to miR-302a inhibitor. Similarly, miR-302a mimic protected hiPSC-CMs against necrosis and apoptosis following SI/RO under NG as well as HG conditions by repressing PTEN with concurrent restoration of phosphorylation of AKT (Ser^{473}). Taken together, these results suggest that reperfusion therapy with RAPA offers robust infarct-sparing benefits with preservation of cardiac function in diabetic rabbits through induction of miR-302a and mTOR-PTEN-AKT signaling pathway.

Role of mTOR Signaling in Cardioprotection

Rapamycin (Everolimus) eluting stents have been successfully used in clinical trials to prevent restenosis and to reduce lumen volume post-acute MI in both diabetic and non-diabetic patients (Dibra et al., 2005;

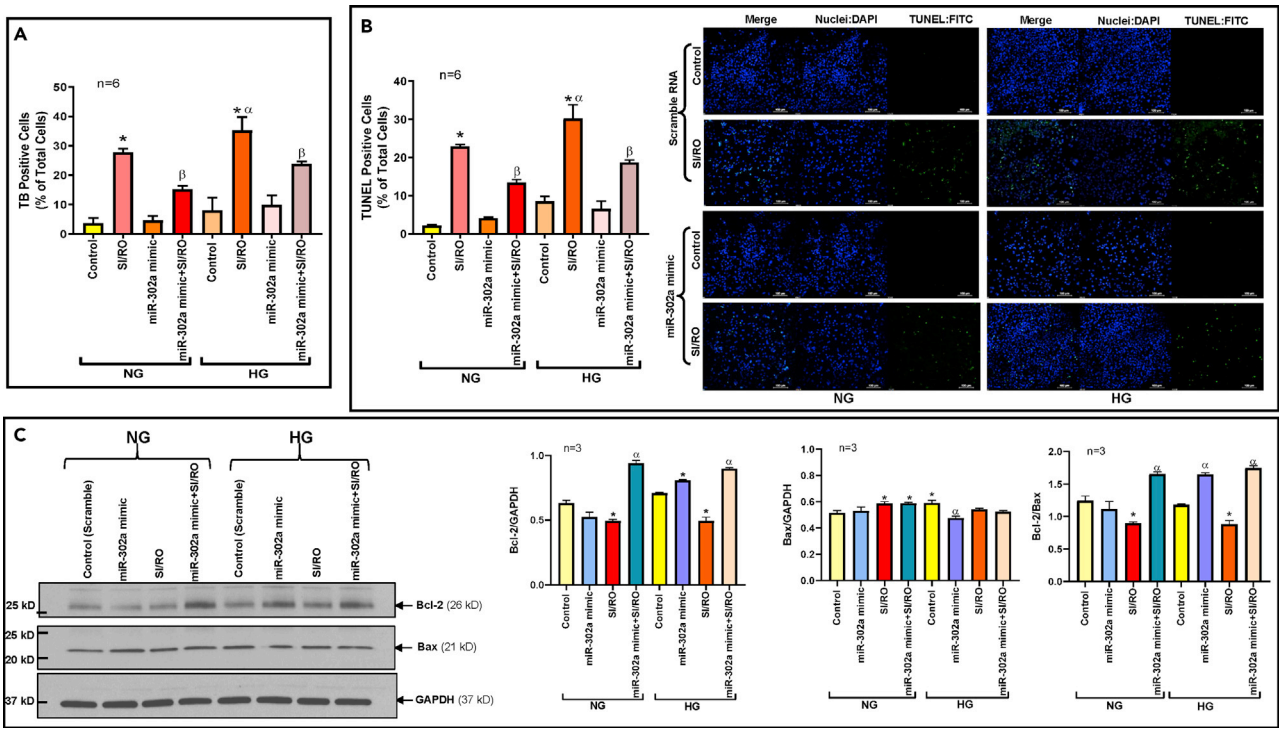

Figure 7. miR-302a Mimic Protects hiPSC-CMs Against Simulated Ischemia and Reoxygenation (SI/RO) Injury Under Normal (NG) and High Glucose (HG) Conditions

(A) Necrosis of hiPSC-CMs transfected with miR-302a mimic and following SI/RO injury under NG and HG conditions. n = 6; *p < 0.0001 versus others; $^{\alpha}$p<0.01 versus SI/RO (NG); $^{\beta}$p<0.001 versus SI/RO (NG & HG).

(B) Apoptosis with representative pictures of TUNEL-DAPI staining in hiPSC-CMs transfected with miR-302a mimic and following SI/RO injury under NG and HG conditions. n = 6; *p < 0.0001 versus others; $^{\alpha}$p<0.01 versus SI/RO (NG); $^{\beta}$p<0.001 versus SI/RO (NG & HG). Scale indicates 100 μm.

(C) Representative immunoblots showing the effect of miR-302a overexpression on expression of Bcl-2 and Bax in hiPSC-CMs following SI/RO under NG and HG conditions. Right panel shows the densitometry analysis of Bcl-2 to GAPDH (n = 3; *p < 0.005 versus control (NG & HG)); $^{\alpha}$p<0.005 versus control & SI/RO (NG & HG)); Bax to GAPDH (n = 3; *p < 0.05 versus control (NG); $^{\alpha}$p<0.05 versus control (HG) & SI/RO (NG & HG)) and Bcl-2 to Bax ratio (n = 3; *p < 0.05 versus control (NG & HG); $^{\alpha}$p<0.005 versus SI/RO (NG & HG). Statistics: one-way ANOVA. Data are represented as mean ± SEM.

Gada et al., 2013; Serruys et al., 2015). However, the acute effect of RAPA in limiting infarct size after MI has never been considered for clinical trial due to paucity of mechanistic insights into mTOR regulation. Using clinically relevant model of I/R in conscious diabetic rabbit, we show that infusion of RAPA following ischemia improved post-I/R survival (mortality in DM + I/R: 21.7%; in DM + I/R + RAPA: 0%) with reduction of infarct size, plasma cTnI release, and oxidative stress as well as restoration of cardiac function. In diabetic mice, we previously demonstrated the upregulation of several antioxidant proteins following RAPA treatment, which was associated with improvement of myocardial function (Das et al., 2014; Filippone et al., 2017). There were no significant changes in hemodynamics during reperfusion, suggesting that RAPA was well tolerated in the diabetic rabbits. Interestingly, LV systolic function at 72 h post-MI was significantly preserved in RAPA-treated diabetic rabbits compared with I/R and DM + I/R groups. Consistent with the infarct-limiting effect of RAPA, myocardial apoptosis was also reduced with RAPA treatment, with associated increase of Bcl-2 expression and subsequent Bcl-2/Bax ratio.

The mTOR–AKT pathway is critical for cell survival and anti-apoptotic signaling and plays an important role in cardioprotection (Datta et al., 1999; Filippone et al., 2017). The mTOR complex is activated by stimuli including insulin, glucose, and nutrients via PI3-PDK kinase mechanism and regulates various downstream targets. mTOR inhibition with RAPA was effective in alleviating LV remodeling and limiting infarct size following MI and pressure overload (Buss et al., 2009; McMullen et al., 2004). The mTORC1 phosphorylates S6K389, which results in enhanced protein synthesis, whereas mTORC2 phosphorylates AKT(Ser^{473}) and can regulate cellular events like apoptosis (Laplante and Sabatini, 2012). Genetic

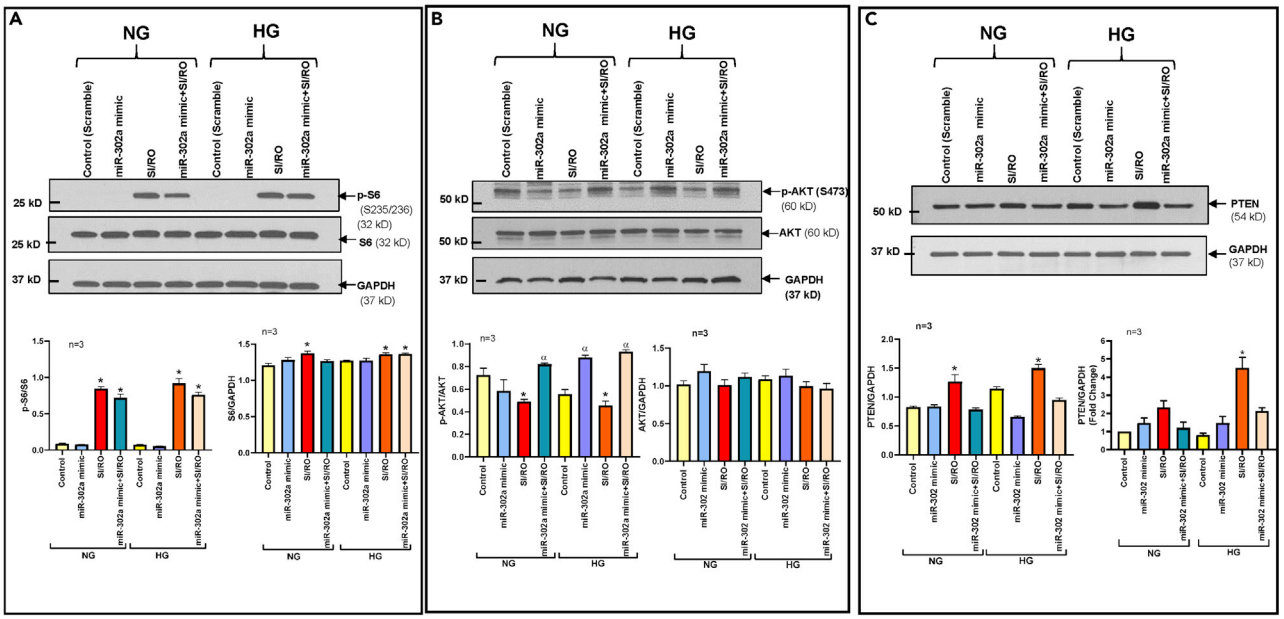

Figure 8. miR-302a Regulates PTEN-AKT-mTORC2 Signaling in hiPSC-CMs Under Normal (NG) and High Glucose (HG) Conditions

(A) Representative Immunoblots showing the effect of overexpression of miR-302a on expression of phosphorylation of S6 in hiPSC-CMs following SI/RO under NG and HG conditions. Bottom panel presents the densitometry analysis (n = 3) of pS6/S6; *p < 0.005 versus control & miR-302 mimic (NG & HG) and S6/GAPDH; *p < 0.05 versus control (NG).

(B) Representative immunoblots showing the phosphorylation level of AKT in hiPSC-CMs transfected with miR-302a mimic following SI/RO under NG and HG conditions. Bottom panel presents the densitometry analysis (n = 3) of pAKT/AKT; *p < 0.005 versus miR-302a mimic + SI/RO (NG & HG); $^{\alpha}$p<0.05 versus control (HG) and AKT/GAPDH.

(C) PTEN expression in hiPSC-CMs transfected with miR-302a mimic following SI/RO under NG and HG conditions. Lower left panel shows densitometry analysis of PTEN with GAPDH as loading control (n = 3; *p < 0.005 versus others). Lower right panel presents real-time PCR analysis of PTEN mRNA in hiPSC-CMs transfected with miR-302a mimic following SI/RO under NG and HG conditions. n = 3; *<0.0001 versus others. Statistics: one-way ANOVA. Data are represented as mean ± SEM.

inactivation or pharmacological inhibition of mTORC1 activates AKT by preventing a negative feedback loop through mTORC1–S6K-induced phosphorylation of insulin receptor substrate via mTORC2 (Song et al., 2012). The acute treatment with RAPA effectively inhibits mTORC1, whereas chronic treatment leads to inhibition of both mTORC1 as well as mTORC2 (Sarbassov et al., 2006). We previously demonstrated that chronic treatment with low-dose RAPA (0.25 mg/kg; 4 weeks) prevented cardiac dysfunction in type 2 diabetic (T2D) mice with inhibition of mTORC1, without impacting mTORC2 (Das et al., 2014). Chronic treatment with RAPA and Rapatar, nanoformulated micelles of RAPA, improved the metabolic status and cardiac function as well as reduced myocardial infarct size following I/R in diabetic mice (Samidurai et al., 2017, 2019). Similarly, chronic treatment with RAPA for 2 weeks markedly reduced infarct size, apoptosis, and improved cardiac function following I/R injury in hypertrophic heart (Ma et al., 2018). Moreover, mTOR phosphorylation and ribosomal protein S6 expression were reduced without changes in AKT in hypertrophied mice (Ma et al., 2018). However, the role of miRNA in RAPA-induced activation/restoration of mTORC2-AKT signaling during reperfusion in diabetic heart has never been investigated.

In the present study, we observed enhanced activation of mTORC1 (phosphorylation of S6 kinase), but inhibition of mTORC2 (phosphorylation of AKT at Ser^{473}) following I/R injury in control hearts, whereas these were more prominent in diabetic rabbit hearts. Treatment with RAPA at reperfusion blunted S6 phosphorylation, but restored AKT phosphorylation in diabetic hearts. These data are consistent with our previous findings and others (Das et al., 2014, 2015; Samidurai et al., 2017, 2019) that inhibiting mTORC1 while simultaneously activating mTORC2 complex with RAPA are cardioprotective in diabetes. Interestingly, selective depletion of Raptor or mTORC1 inhibition with PRAS40 by AAV gene transfer in conjunction with potentiation of mTORC2 led to decreased cardiomyocyte apoptosis and tissue damage after MI (Volkers et al., 2013). This approach also prevented the development of diabetic cardiomyopathy with improved

metabolic function, blunted hypertrophic growth, and preserved cardiac function (Volkers et al., 2014). The present study suggests that the inhibition of mTORC1 with concurrent activation of mTORC2 protected diabetic hearts against reperfusion injury.

Several lines of evidences indicated that the induction of autophagy is associated with cardioprotection in ischemic and pharmacological preconditioning against I/R injury, Funnecessary cytoplasmic proteins or damaged organelles are degraded and ATP production and intracellular homeostasis are maintained with inhibition of apoptotic cell death (Gurusamy et al., 2010; Kubli et al., 2013; Yan et al., 2013). Although myocardial autophagy is elevated in a murine model of T2D, it is suppressed in T1D mice (Mellor et al., 2011; Xie et al., 2011). Multiple studies reported that diabetes did not increase the extent of autophagy in the heart following persistent ischemia (French et al., 2011; Mellor et al., 2013). By blocking the inhibitory effect of mTOR, RAPA induces autophagy and protects cardiomyocytes against pathological conditions involving mitochondrial-generated oxidative stress-induced toxicity (Dutta et al., 2013). It has been shown that RAPA alleviates cardiac I/R injury by inducing PI3K/AKT-mediated autophagy signaling pathway (Wang et al., 2015), but another study reported that RAPA-induced cardioprotection is associated with activation of PI3K and opening of the mitochondrial ATP-sensitive potassium channels, independent of RAPA-induced autophagy (Yang et al., 2010). Future in-depth investigations are needed to understand the interplay between PI3K/AKT activation and autophagy in RAPA-induced protection of diabetic hearts/HG exposed iPSC-CMs against I/R injury.

miR-302a Regulates PTEN-AKT-mTOR Pathway in Diabetic Heart

In the present study, we identified miR-302a (within 12 annotated miRNAs in rabbit, Table S2A), which was significantly suppressed following I/R injury. Multiple sequence alignment performed using R-coffee (http://tcoffee.crg.cat) demonstrated the presence of consensus sequence of miR-302a between human, rabbit, and mouse (Table S2B). Intriguingly, treatment with RAPA restored miR-302a following I/R in diabetic hearts. Based on the bioinformatics evidence, we identified PTEN as one of the potential targets of miR-302a. Mechanistically, PTEN inhibits AKT and plays role in apoptosis, hypertrophy, contractility, and metabolism, which is mediated through mTOR complexes (Oudit et al., 2004). Inducible cardiac-specific PTEN inactivation exerts protection against I/R injury by upregulating anti-apoptotic signals (Ruan et al., 2009). PTEN is modulated during I/R injury and ischemic preconditioning represses PTEN activity, leading to cardioprotection via the transient upregulation of AKT activity during reperfusion (Cai and Semenza, 2005). Impaired pro-survival PTEN-AKT signaling is an important feature of myocardium in diabetic patients, rendering them resistant to preconditioning (Wang et al., 2011). PTEN expression is significantly higher in atrial tissue of patients with T2D, which results in simultaneous reductions in AKT phosphorylation and Bcl-2 expression (Wang et al., 2011). In the present study, there was robust induction of PTEN transcript and protein levels following I/R in diabetic hearts with concurrent reduction of AKT phosphorylation, which was associated with significant suppression of miR-302a. Quite interestingly, treatment with RAPA restored miR-302a levels following I/R injury with coordinated repression of PTEN and restoration of phosphorylation of AKT.

Regulation of miR-302a-PTEN-AKT Signaling in hiPSC-CMs

Although animal models have proven invaluable in uncovering fundamental biology, often they fail to fully mimic the human physiology or recapitulate disease states due to inherent differences between human and rodent biology (Mathur et al., 2013). Therefore, to recapitulate the human relevance of these findings in diabetic rabbit, we further investigated the role of miR-302a-mTOR-PTEN-AKT signaling in RAPA-induced protection in hiPSC-CMs. hiPSC-CMs offer an exceptional opportunity to identify unique therapeutic modalities or underlying mechanisms of human cardiovascular diseases (Martins et al., 2014) because these cells beat spontaneously in culture and possess several phenotypes similar to human cardiomyocyte. Several critical biological processes including oxidative stress, apoptosis as well as aging are regulated through PTEN-AKT signaling and miR-302a, which is predominantly expressed in hiPSC, and induces AKT activation through silencing PTEN (Li et al., 2016). Moreover, hiPSC-CMs offer a superior model for evaluating efficacy of novel drugs for promising therapeutic approaches (Denning et al., 2016; Gintant et al., 2017). Our results showed that cell death following SI/RO was exacerbated under HG condition and treatment with RAPA at re-oxygenation protected hiPSC-CMs by reducing necrosis and apoptosis. Similar to diabetic heart, the decline of miR-302a in hiPSC-CMs following SI/RO was more prominent under HG condition, which was rescued by RAPA, with associated downregulation of PTEN. Interestingly, miR-302a inhibitor abolished the protective effect of the RAPA against SI/RO injury in hiPSC-CMs under

NG/HG conditions by blocking the inhibition of PTEN, induction of AKT phosphorylation and Bcl-2/Bax ratio. Furthermore, the inhibition of S6 phosphorylation with RAPA was insensitive to the miR-302a inhibitor. Similarly, miR-302a mimic protected hiPSC-CMs against SI/RO injury under NG/HG conditions by suppressing PTEN and restoring AKT phosphorylation. However, the protection with miR-302a mimic was less robust compared with RAPA-induced protection of hiPSC-CMs against SI/RO injury, because miR-302a mimic did not inhibit the post-SI/RO activation of mTORC1 (S6 phosphorylation). The data presented in this study elucidate the salutary effect of RAPA against I/R injury in diabetes, which is attributed through miR-302a-mTOR-PTEN-AKT signaling.

Rabbit Model of Diabetes

We used conscious myocardial I/R injury model in T1D rabbits, which has several advantages over rodents. Even though classified as small animal, phylogenetically rabbit (*Oryctolagus cuniculus*) is much closer to humans than mice and rats (Graur et al., 1996). Rabbit strains have a more diverse genetic background mimicking human genetic diversity for studying complex diseases such as diabetes and for developing unique therapeutic strategies. Rabbit heart closely resembles to human heart in terms of collateral circulation (Seiler et al., 2013). In the current study, we used rigorous methodology including the hemodynamic measurements, specific endpoints, randomization, and strict blinding of personnel. The conscious rabbit myocardial I/R model also avoided the confounding effects of anesthetics as well as the stress imposed by acute opening and closing of the chest for performing coronary artery occlusions. Therefore, this model provides reliable results and represent higher confidence for translational approach.

Limitations of the Study

In the present study, we did not follow-up on the long-term effects of diabetes in rabbit heart. Following 4 weeks of alloxan treatment, there were no detectable differences of LVEF of diabetic rabbits as compared with control (non-diabetic rabbits) before and after I/R. However, we did not measure E/A ratios, which would have provided early indications of diastolic dysfunction in the T1D rabbits. In addition, due to several technical challenges beyond our control, we could not evaluate the role of *in vivo* miR-302a inhibition or overexpression on I/R injury in cardiac-specific miR-302a transgenic or knockout diabetic rabbits. Another limitation is that there may be additional miRs, including miR-17-92 cluster (Danielson et al., 2013; Mogilyansky and Rigoutsos, 2013), which could also regulate PTEN expression and need future investigations. To this context, we recently showed that chronic pretreatment with RAPA in T2D diabetic mouse induced miR-17/20a as well as AKT phosphorylation following I/R injury (Samidurai et al., 2019). However, in the present study, we identified miR-302a as a key component in the regulation of mTORC2-dependent AKT pathway through PTEN regulation induced by RAPA in T1D rabbit hearts following I/R injury. Future studies using unbiased global miRarray need to be performed to identify the regulation of other miRs with mTOR inhibition under diabetic condition.

Translational Perspective

Multiple clinical trials of RAPA and other rapalogs are currently underway for several disease conditions including lymphangioleiomyomatosis (LAM), multiple sclerosis (NCT00095329), ALS (amyotrophic lateral sclerosis; NCT03359538), Sturge-Weber syndrome (SWS; NCT03047980), other metabolism modulating interventions on the elderly (NCT02874924), and T1D (NCT01060605; NCT00014911) (Benedini et al., 2018; Gala-Lopez et al., 2013; Glasgow et al., 2010). In fact, the National Cancer Institute has registered more than 200 clinical trials involving either RAPA or its analog both as monotherapy and as combination treatment for cancer (NCT01698918; NCT00337376; NCT00930930) (Kwitkowski et al., 2010; Motzer et al., 2008; Royce et al., 2018; Zaytseva et al., 2012). Although mTOR inhibitors are promising therapeutic options in immunosuppression and cancer treatment, there are scarce reports of clinical trial in cardiovascular diseases. Uncontrolled high blood glucose during diabetes can cause severe cardiovascular complications but treatment with insulin often exacerbates diabetic cardiomyopathy. In the present study, we have demonstrated that reperfusion therapy with RAPA limits myocardial infarct size and apoptosis in diabetic rabbit. In addition, we have identified the crucial role of miR-302a via mTOR-PTEN-AKT signaling pathway in RAPA-induced cardioprotection against I/R injury in a translationally relevant diabetic rabbit model of conscious MI (summarized in **Graphical abstract**). The results suggest that RAPA can be potentially utilized as strong protective agent against diabetic injury instead of insulin, even under conditions of high blood glucose. The mechanistic studies described here also provide insights to the development of an alternative therapy for reperfusion injury in T1D.

Resource Availability

Lead Contact

Further information and requests for resources and reagents should be directed to and will be fulfilled by the Lead Contact, Dr. Anindita Das (anindita.das@vcuhealth.org).

Materials Availability

This study did not generate new unique reagents.

Data and Code Availability

This study did not generate large-scale datasets. All data generated or analyzed during this study are included in this published article (and in Supplemental Information) or are available from the lead author upon request. All original Western Blots are available in Mendeley Data (https://doi.org/10.17632/vzkpkmjbyd.1)

METHODS

All methods can be found in the accompanying Transparent Methods supplemental file.

SUPPLEMENTAL INFORMATION

Supplemental Information can be found online at https://doi.org/10.1016/j.isci.2020.101863.

ACKNOWLEDGMENTS

This work was supported by Grants from the National Institutes of Health RO1HL124366 (AD & RCK), RO1HL118808, R01CA221813, R01DK120866 (RCK), CCTR (Center for Clinical and Translational Research) Endowment Fund (AD) and VETAR (Value and Efficiency Teaching and Research Project) sponsored by of Virginia Commonwealth University (AD). We acknowledge Massey Cancer Center Core Facility for services and products in support of the research project were generated by the Virginia Commonwealth University Cancer Mouse Models Core Laboratory, supported, in part, with funding to the Massey Cancer Center from NIH-NCI Cancer Center Support Grant P30 CA016059.

AUTHORS CONTRIBUTION

A.D., R.C.K., and A.S. designed experiments. A.D., A.S., R.O., C.C., S.K.R., S.M.F., and D.K. performed experiments and analyzed data. A.D., and A.S. wrote the manuscript. R.C.K. and all other authors edited the document.

DECLARATION OF INTERESTS

Authors have no competing interests.

Received: May 11, 2020
Revised: September 7, 2020
Accepted: November 20, 2020
Published: December 18, 2020

REFERENCES

Arsham, A.M., Howell, J.J., and Simon, M.C. (2003). A novel hypoxia-inducible factor-independent hypoxic response regulating mammalian target of rapamycin and its targets. J. Biol. Chem. *278*, 29655–29660.

Benedini, S., Ermetici, F., Briganti, S., Codella, R., Terruzzi, I., Maffi, P., Caldara, R., Secchi, A., Nano, R., Piemonti, L., et al. (2018). Insulin-mimetic effects of short-term rapamycin in type 1 diabetic patients prior to islet transplantation. Acta Diabetol. *55*, 715–722.

Buss, S.J., Muenz, S., Riffel, J.H., Malekar, P., Hagenmueller, M., Weiss, C.S., Bea, F., Bekeredjian, R., Schinke-Braun, M., Izumo, S., et al. (2009). Beneficial effects of Mammalian target of rapamycin inhibition on left ventricular remodeling after myocardial infarction. J. Am. Coll. Cardiol. *54*, 2435–2446.

Cai, Z., and Semenza, G.L. (2005). PTEN activity is modulated during ischemia and reperfusion: involvement in the induction and decay of preconditioning. Circ. Res. *97*, 1351–1359.

Chung, J., Grammer, T.C., Lemon, K.P., Kazlauskas, A., and Blenis, J. (1994). PDGF- and insulin-dependent pp70S6k activation mediated by phosphatidylinositol-3-OH kinase. Nature *370*, 71–75.

Danielson, L.S., Park, D.S., Rotllan, N., Chamorro-Jorganes, A., Guijarro, M.V., Fernandez-Hernando, C., Fishman, G.I., Phoon, C.K., and Hernando, E. (2013). Cardiovascular dysregulation of miR-17-92 causes a lethal hypertrophic cardiomyopathy and arrhythmogenesis. FASEB J. *27*, 1460–1467.

Das, A., Durrant, D., Koka, S., Salloum, F.N., Xi, L., and Kukreja, R.C. (2014). Mammalian target of rapamycin (mTOR) inhibition with rapamycin improves cardiac function in type 2 diabetic mice:

potential role of attenuated oxidative stress and altered contractile protein expression. J. Biol. Chem. *289*, 4145–4160.

Das, A., Salloum, F.N., Filippone, S.M., Durrant, D.E., Rokosh, G., Bolli, R., and Kukreja, R.C. (2015). Inhibition of mammalian target of rapamycin protects against reperfusion injury in diabetic heart through STAT3 signaling. Basic Res. Cardiol. *110*, 31.

Datta, S.R., Brunet, A., and Greenberg, M.E. (1999). Cellular survival: a play in three Akts. Genes Dev. *13*, 2905–2927.

de Ferranti, S.D., de Boer, I.H., Fonseca, V., Fox, C.S., Golden, S.H., Lavie, C.J., Magge, S.N., Marx, N., McGuire, D.K., Orchard, T.J., et al. (2014). Type 1 diabetes mellitus and cardiovascular disease: a scientific statement from the American Heart Association and American Diabetes Association. Diabetes Care *37*, 2843–2863.

Denning, C., Borgdorff, V., Crutchley, J., Firth, K.S., George, V., Kalra, S., Kondrashov, A., Hoang, M.D., Mosqueira, D., Patel, A., et al. (2016). Cardiomyocytes from human pluripotent stem cells: from laboratory curiosity to industrial biomedical platform. Biochim. Biophys. Acta *1863*, 1728–1748.

Dennis, P.B., Jaeschke, A., Saitoh, M., Fowler, B., Kozma, S.C., and Thomas, G. (2001). Mammalian TOR: a homeostatic ATP sensor. Science *294*, 1102–1105.

Dibra, A., Kastrati, A., Mehilli, J., Pache, J., Schuhlen, H., von, B.N., Ulm, K., Wessely, R., Dirschinger, J., and Schomig, A. (2005). Paclitaxel-eluting or sirolimus-eluting stents to prevent restenosis in diabetic patients. N. Engl. J. Med. *353*, 663–670.

Ding, M., Dong, Q., Liu, Z., Liu, Z., Qu, Y., Li, X., Huo, C., Jia, X., Fu, F., and Wang, X. (2017). Inhibition of dynamin-related protein 1 protects against myocardial ischemia-reperfusion injury in diabetic mice. Cardiovasc. Diabetol. *16*, 19.

Dutta, D., Xu, J., Kim, J.S., Dunn, W.A., Jr., and Leeuwenburgh, C. (2013). Upregulated autophagy protects cardiomyocytes from oxidative stress-induced toxicity. Autophagy *9*, 328–344.

Filippone, S.M., Samidurai, A., Roh, S.K., Cain, C.K., He, J., Salloum, F.N., Kukreja, R.C., and Das, A. (2017). Reperfusion therapy with rapamycin attenuates myocardial infarction through activation of AKT and ERK. Oxid Med. Cell. Longev. *2017*, 4619720.

French, C.J., Tarikuz Zaman, A., McElroy-Yaggy, K.L., Neimane, D.K., and Sobel, B.E. (2011). Absence of altered autophagy after myocardial ischemia in diabetic compared with nondiabetic mice. Coron. Artery Dis. *22*, 479–483.

Gada, H., Kirtane, A.J., Newman, W., Sanz, M., Hermiller, J.B., Mahaffey, K.W., Cutlip, D.E., Sudhir, K., Hou, L., Koo, K., et al. (2013). 5-year results of a randomized comparison of XIENCE V everolimus-eluting and TAXUS paclitaxel-eluting stents: final results from the SPIRIT III trial (clinical evaluation of the XIENCE V everolimus eluting coronary stent system in the treatment of patients with de novo native coronary artery lesions). JACC Cardiovasc. Interv. *6*, 1263–1266.

Gala-Lopez, B., Kin, T., O'Gorman, D., Pepper, A.R., Senior, P., Humar, A., and Shapiro, A.M. (2013). Microbial contamination of clinical islet transplant preparations is associated with very low risk of infection. Diabetes Technol. Ther. *15*, 323–327.

Gintant, G., Fermini, B., Stockbridge, N., and Strauss, D. (2017). The evolving roles of human iPSC-derived cardiomyocytes in drug safety and discovery. Cell Stem Cell *21*, 14–17.

Glasgow, C.G., Steagall, W.K., Taveira-Dasilva, A., Pacheco-Rodriguez, G., Cai, X., El-Chemaly, S., Moses, M., Darling, T., and Moss, J. (2010). Lymphangioleiomyomatosis (LAM): molecular insights lead to targeted therapies. Respir. Med. *104* (*Suppl 1*), S45–S58.

Glass, C., and Singla, D.K. (2011). MicroRNA-1 transfected embryonic stem cells enhance cardiac myocyte differentiation and inhibit apoptosis by modulating the PTEN/Akt pathway in the infarcted heart. Am. J. Physiol. Heart Circ. Physiol. *301*, H2038–H2049.

Graur, D., Duret, L., and Gouy, M. (1996). Phylogenetic position of the order Lagomorpha (rabbits, hares and allies). Nature *379*, 333–335.

Gurusamy, N., Lekli, I., Mukherjee, S., Ray, D., Ahsan, M.K., Gherghiceanu, M., Popescu, L.M., and Das, D.K. (2010). Cardioprotection by resveratrol: a novel mechanism via autophagy involving the mTORC2 pathway. Cardiovasc. Res. *86*, 103–112.

Hinkel, R., Howe, A., Renner, S., Ng, J., Lee, S., Klett, K., Kaczmarek, V., Moretti, A., Laugwitz, K.L., Skroblin, P., et al. (2017). Diabetes mellitus-induced microvascular destabilization in the myocardium. J. Am. Coll. Cardiol. *69*, 131–143.

Jha, J.C., Ho, F., Dan, C., and Jandeleit-Dahm, K. (2018). A causal link between oxidative stress and inflammation in cardiovascular and renal complications of diabetes. Clin. Sci. (Lond) *132*, 1811–1836.

Keyes, K.T., Xu, J., Long, B., Zhang, C., Hu, Z., and Ye, Y. (2010). Pharmacological inhibition of PTEN limits myocardial infarct size and improves left ventricular function postinfarction. Am. J. Physiol. Heart Circ. Physiol. *298*, H1198–H1208.

Kubli, D.A., Zhang, X., Lee, Y., Hanna, R.A., Quinsay, M.N., Nguyen, C.K., Jimenez, R., Petrosyan, S., Murphy, A.N., and Gustafsson, A.B. (2013). Parkin protein deficiency exacerbates cardiac injury and reduces survival following myocardial infarction. J. Biol. Chem. *288*, 915–926.

Kwitkowski, V.E., Prowell, T.M., Ibrahim, A., Farrell, A.T., Justice, R., Mitchell, S.S., Sridhara, R., and Pazdur, R. (2010). FDA approval summary: temsirolimus as treatment for advanced renal cell carcinoma. Oncologist *15*, 428–435.

Laplante, M., and Sabatini, D.M. (2012). mTOR signaling in growth control and disease. Cell *149*, 274–293.

Lejay, A., Fang, F., John, R., Van, J.A., Barr, M., Thaveau, F., Chakfe, N., Geny, B., and Scholey, J.W. (2016). Ischemia reperfusion injury, ischemic conditioning and diabetes mellitus. J. Mol. Cell. Cardiol. *91*, 11–22.

Leslie, N.R., Batty, I.H., Maccario, H., Davidson, L., and Downes, C.P. (2008). Understanding PTEN regulation: PIP2, polarity and protein stability. Oncogene *27*, 5464–5476.

Li, H.H., Lin, S.L., Huang, C.N., Lu, F.J., Chiu, P.Y., Huang, W.N., Lai, T.J., and Lin, C.L. (2016). miR-302 attenuates amyloid-beta-induced neurotoxicity through activation of akt signaling. J. Alzheimers Dis. *50*, 1083–1098.

Ling, S., Birnbaum, Y., Nanhwan, M.K., Thomas, B., Bajaj, M., Li, Y., Li, Y., and Ye, Y. (2013). Dickkopf-1 (DKK1) phosphatase and tensin homolog on chromosome 10 (PTEN) crosstalk via microRNA interference in the diabetic heart. Basic Res. Cardiol. *108*, 352.

Loewith, R., Jacinto, E., Wullschleger, S., Lorberg, A., Crespo, J.L., Bonenfant, D., Oppliger, W., Jenoe, P., and Hall, M.N. (2002). Two TOR complexes, only one of which is rapamycin sensitive, have distinct roles in cell growth control. Mol. Cell *10*, 457–468.

Ma, L.L., Ma, X., Kong, F.J., Guo, J.J., Shi, H.T., Zhu, J.B., Zou, Y.Z., and Ge, J.B. (2018). Mammalian target of rapamycin inhibition attenuates myocardial ischaemia-reperfusion injury in hypertrophic heart. J. Cell. Mol. Med. *22*, 1708–1719.

Margeirsdottir, H.D., Larsen, J.R., Brunborg, C., Overby, N.C., and Dahl-Jorgensen, K. (2008). High prevalence of cardiovascular risk factors in children and adolescents with type 1 diabetes: a population-based study. Diabetologia *51*, 554–561.

Martins, A.M., Vunjak-Novakovic, G., and Reis, R.L. (2014). The current status of iPS cells in cardiac research and their potential for tissue engineering and regenerative medicine. Stem Cell Rev. *10*, 177–190.

Mathur, A., Loskill, P., Hong, S., Lee, J., Marcus, S.G., Dumont, L., Conklin, B.R., Willenbring, H., Lee, L.P., and Healy, K.E. (2013). Human induced pluripotent stem cell-based microphysiological tissue models of myocardium and liver for drug development. Stem Cell Res. Ther. *4* (*Suppl 1*), S14.

Mayer-Davis, E.J., Lawrence, J.M., Dabelea, D., Divers, J., Isom, S., Dolan, L., Imperatore, G., Linder, B., Marcovina, S., Pettitt, D.J., et al. (2017). Incidence trends of type 1 and type 2 diabetes among youths, 2002-2012. N. Engl. J. Med. *376*, 1419–1429.

McMullen, J.R., Sherwood, M.C., Tarnavski, O., Zhang, L., Dorfman, A.L., Shioi, T., and Izumo, S. (2004). Inhibition of mTOR signaling with rapamycin regresses established cardiac hypertrophy induced by pressure overload. Circulation *109*, 3050–3055.

Mellor, K.M., Bell, J.R., Ritchie, R.H., and Delbridge, L.M. (2013). Myocardial insulin resistance, metabolic stress and autophagy in diabetes. Clin. Exp. Pharmacol. Physiol. *40*, 56–61.

Mellor, K.M., Reichelt, M.E., and Delbridge, L.M. (2011). Autophagy anomalies in the diabetic myocardium. Autophagy *7*, 1263–1267.

Miki, T., Itoh, T., Sunaga, D., and Miura, T. (2012). Effects of diabetes on myocardial infarct size and

cardioprotection by preconditioning and postconditioning. Cardiovasc. Diabetol. *11*, 67.

Mogilyansky, E., and Rigoutsos, I. (2013). The miR-17/92 cluster: a comprehensive update on its genomics, genetics, functions and increasingly important and numerous roles in health and disease. Cell Death Differ. *20*, 1603–1614.

Motzer, R.J., Escudier, B., Oudard, S., Hutson, T.E., Porta, C., Bracarda, S., Grunwald, V., Thompson, J.A., Figlin, R.A., Hollaender, N., et al. (2008). Efficacy of everolimus in advanced renal cell carcinoma: a double-blind, randomised, placebo-controlled phase III trial. Lancet *372*, 449–456.

Oudit, G.Y., Kassiri, Z., Zhou, J., Liu, Q.C., Liu, P.P., Backx, P.H., Dawood, F., Crackower, M.A., Scholey, J.W., and Penninger, J.M. (2008). Loss of PTEN attenuates the development of pathological hypertrophy and heart failure in response to biomechanical stress. Cardiovasc. Res. *78*, 505–514.

Oudit, G.Y., Sun, H., Kerfant, B.G., Crackower, M.A., Penninger, J.M., and Backx, P.H. (2004). The role of phosphoinositide-3 kinase and PTEN in cardiovascular physiology and disease. J. Mol. Cell Cardiol. *37*, 449–471.

Parajuli, N., Yuan, Y., Zheng, X., Bedja, D., and Cai, Z.P. (2012). Phosphatase PTEN is critically involved in post-myocardial infarction remodeling through the Akt/interleukin-10 signaling pathway. Basic Res. Cardiol. *107*, 248.

Park, L., Raman, K.G., Lee, K.J., Lu, Y., Ferran, L.J., Jr., Chow, W.S., Stern, D., and Schmidt, A.M. (1998). Suppression of accelerated diabetic atherosclerosis by the soluble receptor for advanced glycation endproducts. Nat. Med. *4*, 1025–1031.

Pulido, R. (2018). PTEN inhibition in human disease therapy. Molecules *23*, E285.

Royce, M., Bachelot, T., Villanueva, C., Ozguroglu, M., Azevedo, S.J., Cruz, F.M., Debled, M., Hegg, R., Toyama, T., Falkson, C., et al. (2018). Everolimus plus endocrine therapy for postmenopausal women with estrogen receptor-positive, human epidermal growth factor receptor 2-negative advanced breast cancer: a clinical trial. JAMA Oncol. *4*, 977–984.

Ruan, H., Li, J., Ren, S., Gao, J., Li, G., Kim, R., Wu, H., and Wang, Y. (2009). Inducible and cardiac specific PTEN inactivation protects ischemia/reperfusion injury. J. Mol. Cell Cardiol. *46*, 193–200.

Samidurai, A., Roh, S.K., Prakash, M., Durrant, D., Salloum, F.N., Kukreja, R.C., and Das, A. (2019). STAT3-miR-17/20 signaling Axis plays a critical role in attenuating myocardial infarction following rapamycin treatment in diabetic mice. Cardiovasc. Res. cvz315.

Samidurai, A., Salloum, F.N., Durrant, D., Chernova, O.B., Kukreja, R.C., and Das, A. (2017). Chronic treatment with novel nanoformulated micelles of rapamycin, Rapatar, protects diabetic heart against ischaemia/reperfusion injury. Br. J. Pharmacol. *174*, 4771–4784.

Sarbassov, D.D., Ali, S.M., Sengupta, S., Sheen, J.H., Hsu, P.P., Bagley, A.F., Markhard, A.L., and Sabatini, D.M. (2006). Prolonged rapamycin treatment inhibits mTORC2 assembly and Akt/PKB. Mol. Cell *22*, 159–168.

Sayed, D., He, M., Hong, C., Gao, S., Rane, S., Yang, Z., and Abdellatif, M. (2010). MicroRNA-21 is a downstream effector of AKT that mediates its antiapoptotic effects via suppression of Fas ligand. J. Biol. Chem. *285*, 20281–20290.

Seiler, C., Stoller, M., Pitt, B., and Meier, P. (2013). The human coronary collateral circulation: development and clinical importance. Eur. Heart J. *34*, 2674–2682.

Serruys, P.W., Chevalier, B., Dudek, D., Cequier, A., Carrie, D., Iniguez, A., Dominici, M., van der Schaaf, R.J., Haude, M., Wasungu, L., et al. (2015). A bioresorbable everolimus-eluting scaffold versus a metallic everolimus-eluting stent for ischaemic heart disease caused by de-novo native coronary artery lesions (ABSORB II): an interim 1-year analysis of clinical and procedural secondary outcomes from a randomised controlled trial. Lancet *385*, 43–54.

Severino, P., D'Amato, A., Netti, L., Pucci, M., Infusino, F., Maestrini, V., Mancone, M., and Fedele, F. (2019). Myocardial ischemia and diabetes mellitus: role of oxidative stress in the connection between cardiac metabolism and coronary blood flow. J. Diabetes Res. *2019*, 9489826.

Shang, L., Ananthakrishnan, R., Li, Q., Quadri, N., Abdillahi, M., Zhu, Z., Qu, W., Rosario, R., Toure, F., Yan, S.F., et al. (2010). RAGE modulates hypoxia/reoxygenation injury in adult murine cardiomyocytes via JNK and GSK-3beta signaling pathways. PLoS One *5*, e10092.

Sima, A.V., Botez, G.M., Stancu, C.S., Manea, A., Raicu, M., and Simionescu, M. (2010). Effect of irreversibly glycated LDL in human vascular smooth muscle cells: lipid loading, oxidative and inflammatory stress. J. Cell. Mol. Med. *14*, 2790–2802.

Song, M.S., Salmena, L., and Pandolfi, P.P. (2012). The functions and regulation of the PTEN tumour suppressor. Nat. Rev. Mol. Cell Biol. *13*, 283–296.

Stamateris, R.E., Sharma, R.B., Kong, Y., Ebrahimpour, P., Panday, D., Ranganath, P., Zou, B., Levitt, H., Parambil, N.A., O'Donnell, C.P., et al. (2016). Glucose induces mouse beta-cell proliferation via IRS2, MTOR, and cyclin D2 but not the insulin receptor. Diabetes *65*, 981–995.

Thoreen, C.C., Chantranupong, L., Keys, H.R., Wang, T., Gray, N.S., and Sabatini, D.M. (2012). A unifying model for mTORC1-mediated regulation of mRNA translation. Nature *485*, 109–113.

Tian, Y., Liu, Y., Wang, T., Zhou, N., Kong, J., Chen, L., Snitow, M., Morley, M., Li, D., Petrenko, N., et al. (2015). A microRNA-Hippo pathway that promotes cardiomyocyte proliferation and cardiac regeneration in mice. Sci. Transl Med. *7*, 279ra238.

Ungurianu, A., Margina, D., Gradinaru, D., Bacanu, C., Ilie, M., Tsitsimpikou, C., Tsarouhas, K., Spandidos, D.A., and Tsatsakis, A.M. (2017). Lipoprotein redox status evaluation as a marker of cardiovascular disease risk in patients with inflammatory disease. Mol. Med. Rep. *15*, 256–262.

Volkers, M., Doroudgar, S., Nguyen, N., Konstandin, M.H., Quijada, P., Din, S., Ornelas, L., Thuerauf, D.J., Gude, N., Friedrich, K., et al. (2014). PRAS40 prevents development of diabetic cardiomyopathy and improves hepatic insulin sensitivity in obesity. EMBO Mol. Med. *6*, 57–65.

Volkers, M., Konstandin, M.H., Doroudgar, S., Toko, H., Quijada, P., Din, S., Joyo, A., Ornelas, L., Samse, K., Thuerauf, D.J., et al. (2013). Mechanistic target of rapamycin complex 2 protects the heart from ischemic damage. Circulation *128*, 2132–2144.

Wang, B., Raedschelders, K., Shravah, J., Hui, Y., Safaei, H.G., Chen, D.D., Cook, R.C., Fradet, G., Au, C.L., and Ansley, D.M. (2011). Differences in myocardial PTEN expression and Akt signalling in type 2 diabetic and nondiabetic patients undergoing coronary bypass surgery. Clin. Endocrinol. (Oxf) *74*, 705–713.

Wang, L.Q., Cheng, X.S., Huang, C.H., Huang, B., and Liang, Q. (2015). Rapamycin protects cardiomyocytes against anoxia/reoxygenation injury by inducing autophagy through the PI3k/Akt pathway. J. Huazhong Univ. Sci. Technol. Med. Sci. *35*, 10–15.

Wang, X., Zhang, X., Ren, X.P., Chen, J., Liu, H., Yang, J., Medvedovic, M., Hu, Z., and Fan, G.C. (2010). MicroRNA-494 targeting both proapoptotic and antiapoptotic proteins protects against ischemia/reperfusion-induced cardiac injury. Circulation *122*, 1308–1318.

Xie, Z., Lau, K., Eby, B., Lozano, P., He, C., Pennington, B., Li, H., Rathi, S., Dong, Y., Tian, R., et al. (2011). Improvement of cardiac functions by chronic metformin treatment is associated with enhanced cardiac autophagy in diabetic OVE26 mice. Diabetes *60*, 1770–1778.

Yan, W.J., Dong, H.L., and Xiong, L.Z. (2013). The protective roles of autophagy in ischemic preconditioning. Acta Pharmacol. Sin. *34*, 636–643.

Yang, S.S., Liu, Y.B., Yu, J.B., Fan, Y., Tang, S.Y., Duan, W.T., Wang, Z., Gan, R.T., and Yu, B. (2010). Rapamycin protects heart from ischemia/reperfusion injury independent of autophagy by activating PI3 kinase-Akt pathway and mitochondria K(ATP) channel. Pharmazie *65*, 760–765.

Yano, T., Ferlito, M., Aponte, A., Kuno, A., Miura, T., Murphy, E., and Steenbergen, C. (2014). Pivotal role of mTORC2 and involvement of ribosomal protein S6 in cardioprotective signaling. Circ. Res. *114*, 1268–1280.

Yetgin, T., Magro, M., Manintveld, O.C., Nauta, S.T., Cheng, J.M., den Uil, C.A., Simsek, C., Hersbach, F., van Domburg, R.T., Boersma, E., et al. (2014). Impact of multiple balloon inflations during primary percutaneous coronary intervention on infarct size and long-term clinical outcomes in ST-segment elevation myocardial infarction: real-world postconditioning. Basic Res. Cardiol. *109*, 403.

Zaytseva, Y.Y., Valentino, J.D., Gulhati, P., and Evers, B.M. (2012). mTOR inhibitors in cancer therapy. Cancer Lett. *319*, 1–7.

iScience, Volume *23*

Supplemental Information

Differential Regulation of mTOR Complexes with miR-302a Attenuates Myocardial Reperfusion Injury in Diabetes

Arun Samidurai, Ramzi Ockaili, Chad Cain, Sean K. Roh, Scott M. Filippone, Donatas Kraskauskas, Rakesh C. Kukreja, and Anindita Das

Supplemental Information

Table S1.

Parameter	Control (n=7)	I/R (n=7)	DM (n=10)	DM +I/R (n=12)	DM + I/R + RAPA (n=12)
Body Weight (Kg)	3.2 ± 0.08	3.1 ± 0.09	3.2 ± 0.059	3.41 ± 0.079	3.46 ± 0.078
Age (months)	3.4 ± 0.2	3.5 ± 0.6	5.7 ± 0.3	5.8 ± 0.4	5.8 ± 0.2
Blood glucose level (mg/dL)	162 ± 5.75	161 ± 9.78	339 ± 19.5 **	349 ± 16.8 **	337 ± 11.4 **
Heart Weight (g)	9.5 ± 0.35	9.06 ± 0.33	10.12 ± 0.31	11.25 ± 0.22	10.33 ± 0.24
Heart/Body Weight (g/Kg)	2.97 ± 0.07	2.87 ± 0.15	3.17 ± 0.11	3.39 ± 0.11	3.1 ± 0.09

Blood glucose and physiological parameters of rabbits. Related to Figure 1.
Body weight, age, blood glucose and heart/body weight ratio of control, ischemia/reperfusion (I/R), diabetes (DM), diabetes+I/R (DM+I/R) and diabetes+I/R+Rapamycin (DM+I/R+RAPA) groups at the end of the protocol. Values are mean ± SEM. All comparisons were determined using ANOVA + Bonferroni test, **$p<0.0001$ vs Control & I/R.

Table S2.

A **Oryctolagus Cuniculus miRNAs (12 Sequences) OryCun 2.0**

ID	Accession	Chromosome	Start	End	Strand
ocu-mir-191	MI0030998	chr9	16649737	16649828	-
ocu-mir-290	MI0030993				
ocu-mir-294	MI0030992				
ocu-mir-302a	MI0030989	chr15	36769946	36770014	+
ocu-mir-302b	MI0030987	chr15	36769627	36769706	+
ocu-mir-302c	MI0030988	chr15	36769770	36769837	+
ocu-mir-302d	MI0030990	chr15	36770109	36770176	+
ocu-mir-367	MI0030991	chr15	36770233	36770300	+
ocu-mir-498	MI0030995				
ocu-mir-512a	MI0030996				
ocu-mir-512b	MI0030997				
ocu-mir-520e	MI0030994				

B Sequence homology of miR-302a among human, rabbit, mouse and monkey (http://tcoffee.crg.cat)

Accession No	Species	miR Name	miR Sequence
			Seed Region
(MIMAT0000684)	Human	hsa-miR-302a	UAAGUGCUUCCAUGUUUUGGUGA
(MIMAT0036321)	Rabbit	ocu-miR-302a	UAAGUGCUUCCAUGUUUUGGUGA
(MIMAT0000380)	Mouse	mmu-miR-302a	UAAGUGCUUCCAUGUUUUGGUGA
(MIMAT0006259)	Monkey	mml-miR-302a	UAAGUGCUUCCAUGUUUUGGUGA
		cons	**********

http://www.mirbase.org/cgi-bin/query.pl?terms=Oryctolagus+cuniculus&submit=Search

Bioinformatics annotation of microRNAs in Rabbit. Related with Figure 4B and Figure S4.
(A) Details of 12 miRNAs in rabbits. (B) Multiple sequence alignment of miR-302a in human, rabbit, mouse and monkey. * indicates the presence of consensus sequence of miR-302a between human, rabbit, mouse and monkey.

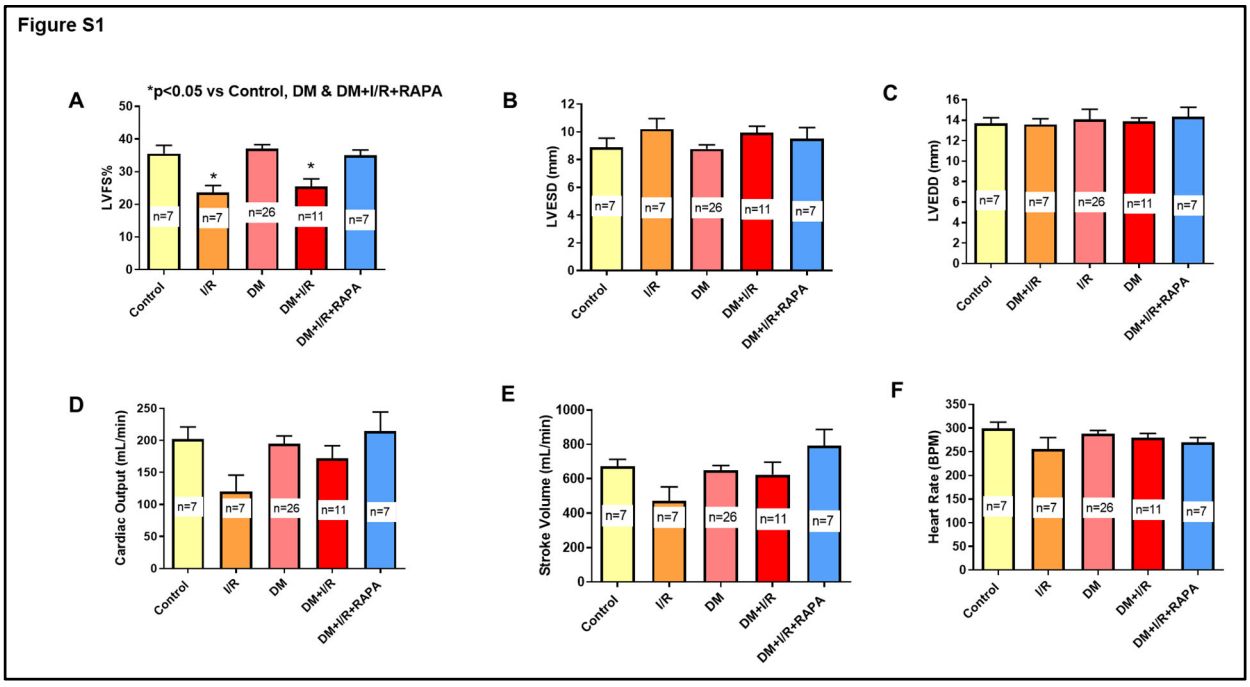

Cardiac function of control and diabetic (DM) rabbits before and after ischemia/reperfusion (I/R) injury with/without rapamycin (RAPA) treatment. Related to Figure 2.

Rabbits were subjected to 45 min conscious I and 72 hours of reperfusion. Diabetic rabbits were treated with RAPA at the onset of reperfusion (DM+I/R+RAPA).

(A) Percentage of left ventricular fractional shortening (LVFS, *p<0.05 vs Control, DM & DM+I/R+RAPA),
(B) LV end systolic diameter (LVESD),
(C) LV end diastolic diameter (LVEDD),
(D) Cardiac output,
(E) Stroke volume,
(F) Heart rate

Statistics: One-way ANOVA. Data are represented as mean ± SEM.

Figure S2

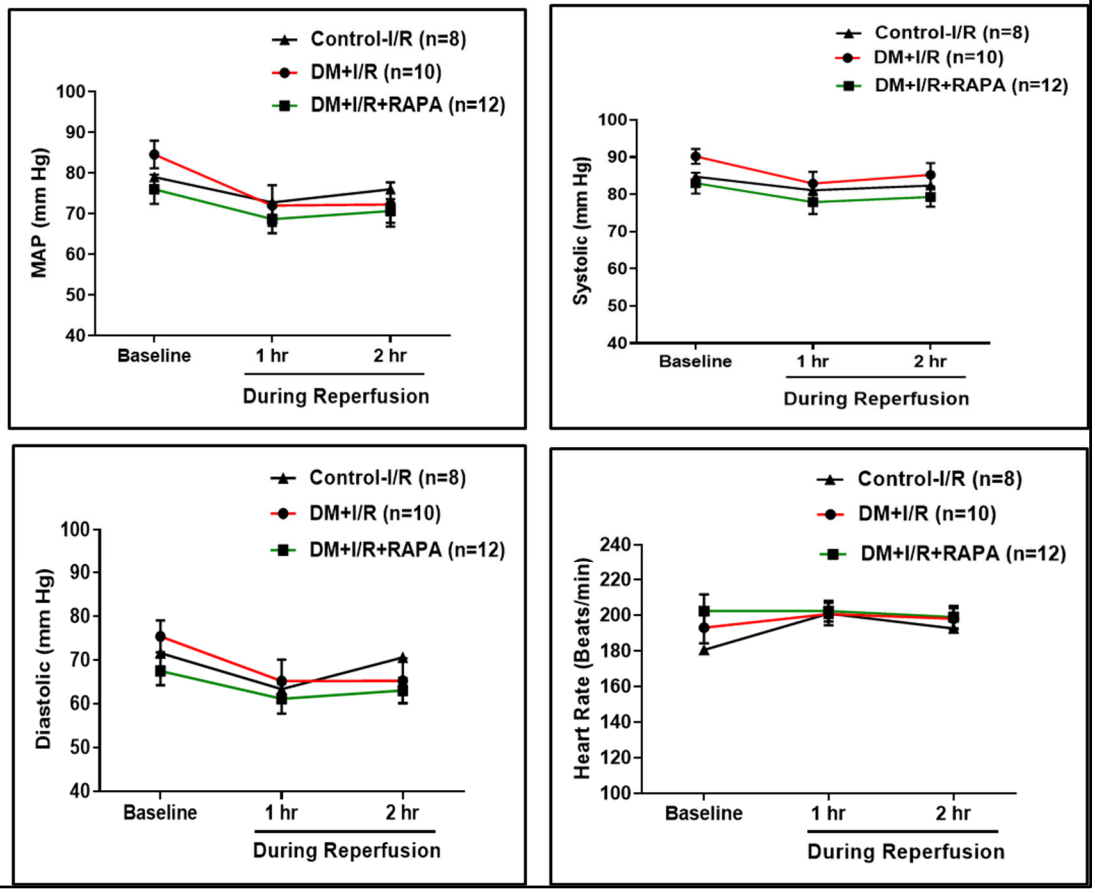

Hemodynamic measurements in control and diabetic rabbits after ischemia/reperfusion (I/R) injury with/without rapamycin (RAPA) treatment. Related to Figure 1B and Figure 2.

(A) Mean Arterial Pressure (MAP);

(B) Systolic Pressure (SBP);

(C) Diastolic Pressure (DBP);

(D) Heart rate (HR) in control (I/R) and diabetic rabbits after I/R (DM+I/R) and with RAPA (DM+I/R+RAPA). Acute administration of RAPA (0.25 mg/kg of BW; i.v.) was well tolerated by rabbits during the treatment procedure and had no significant influence on hemodynamic parameters.

Statistics: One-way ANOVA. Data are represented as mean ± SEM.

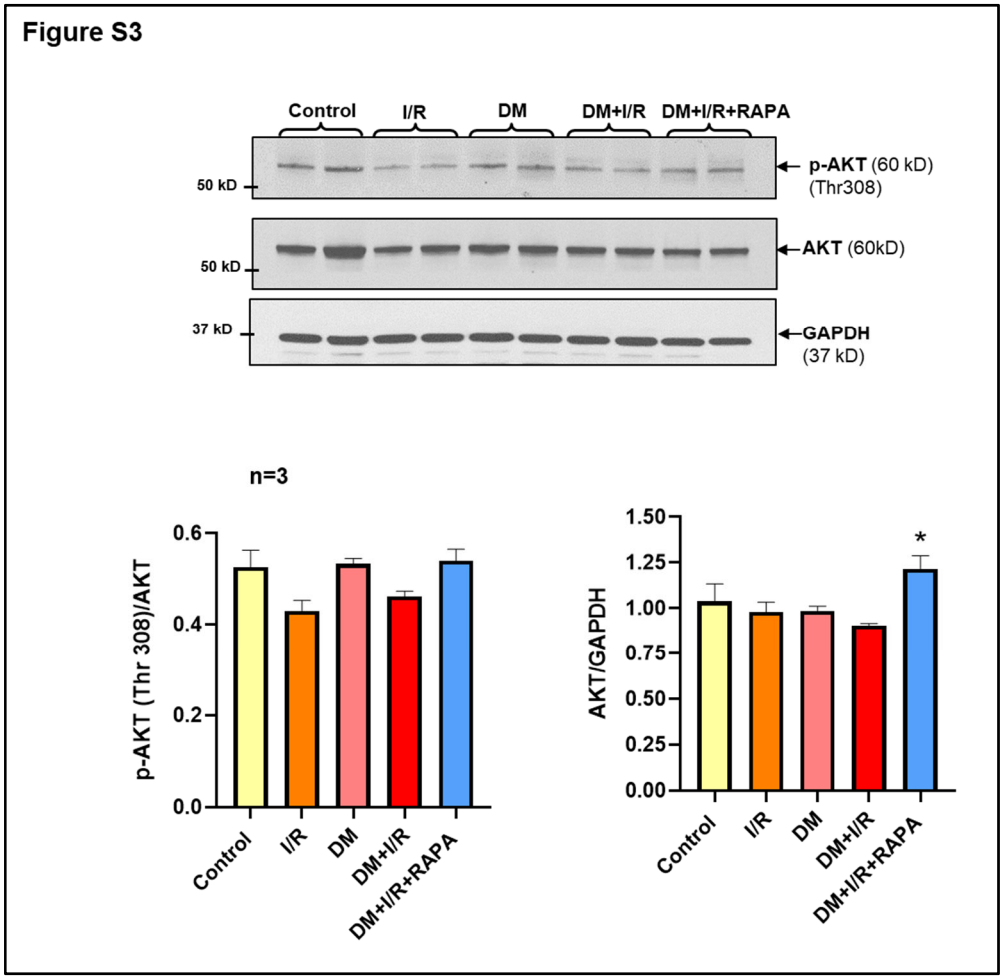

Phosphorylation of AKT at Thr308 in diabetic rabbits following ischemia/reperfusion (I/R) injury with/without rapamycin (RAPA) treatment. Related to Figure 4A.

Upper panel shows the representative immunoblots and lower panel shows densitometry analysis of the ratios of phosphorylation of AKT to total AKT (p-AKT/AKT) and total AKT to GAPDH in control and diabetic rabbit hearts following I/R injury (n=3; *$p<0.05$ vs DM+I/R). Diabetic rabbits were treated with RAPA at the onset of reperfusion (DM+I/R+RAPA).

Statistics: One-way ANOVA. Data are represented as mean ± SEM.

Figure S4

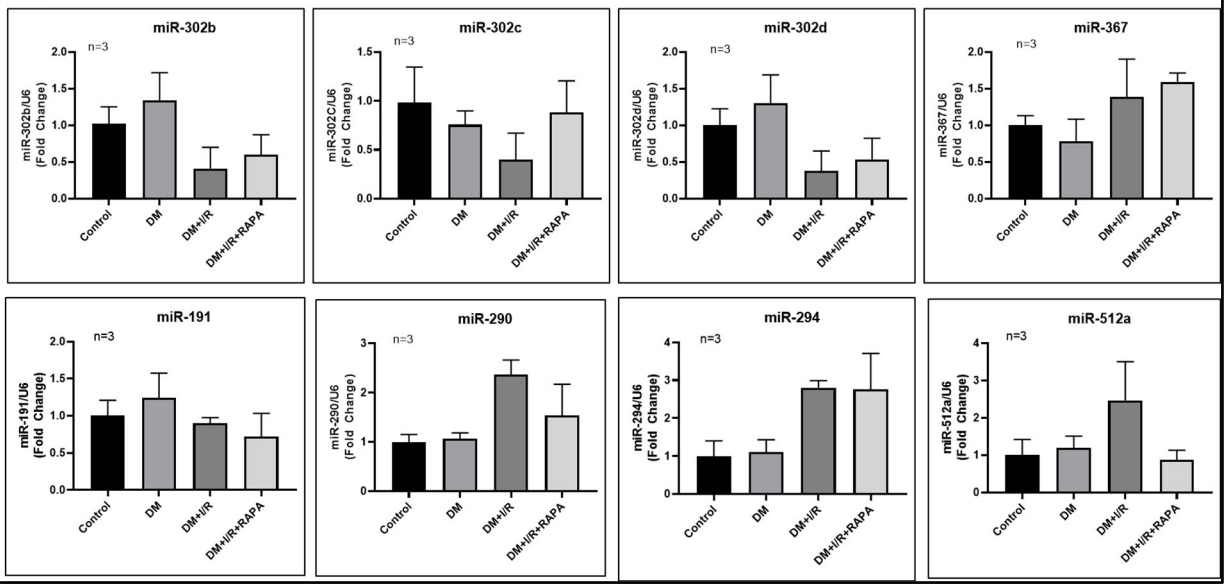

Expression profiles of miRNAs. Related to Figure 4B.
Expression profiles of miR-302b, miR-302c, miR-302d, miR-367, miR-191, miR-290, miR-294 and miR-512a in hearts of control and diabetic rabbits (DM) with/without rapamycin (RAPA) treatment during reperfusion.
Statistics: One-way ANOVA. Data are represented as mean ± SEM.

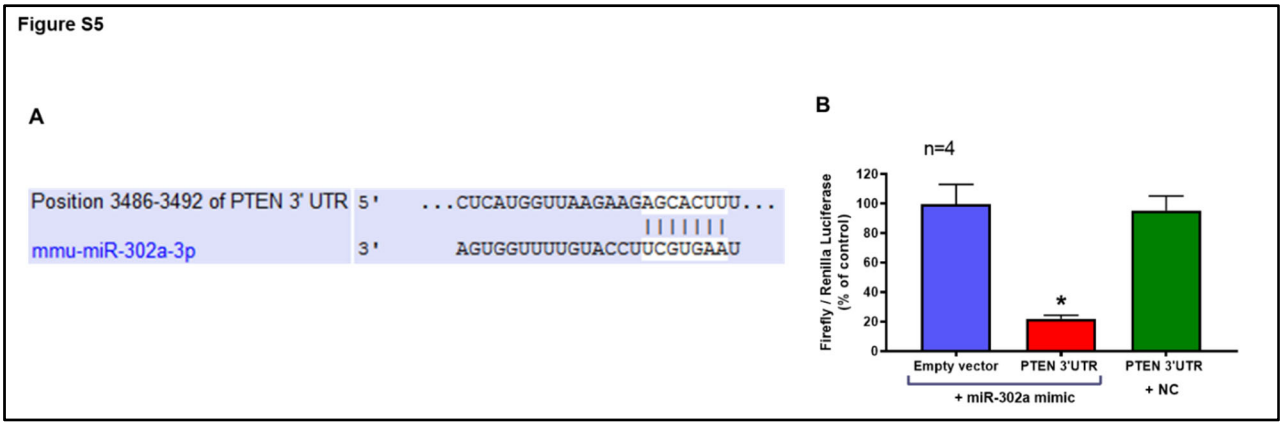

Interaction between miR-302a and 3'UTR of PTEN. Related to Figure 4C and D, 6D and 8C.
A. Prediction of two binding sites for mmu-miR-302a-3p in the 3′-UTR (untranslated region) of PTEN.

B. Dual-luciferase assays showed that the reduction of luciferase activity with the 3'-UTR of PTEN with mimic of miR-302a compared with the negative control (NC) of miR-302a binding site. n=4; *p<0.001 vs others.

Statistics: One-way ANOVA. Data are represented as mean ± SEM.

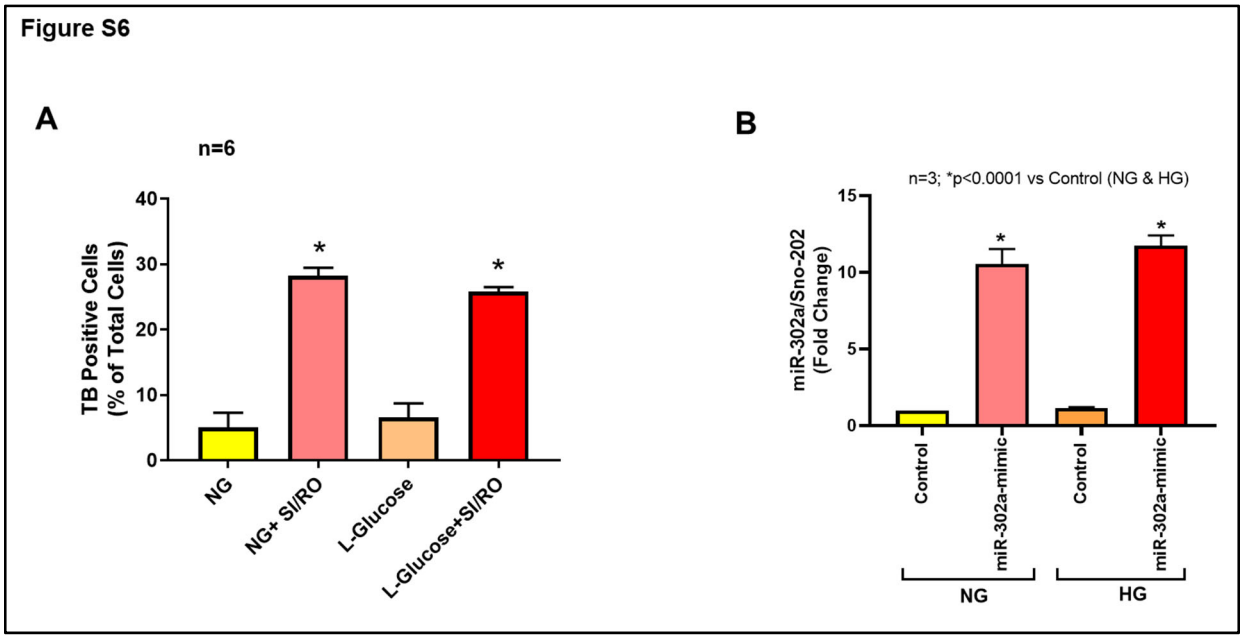

A. Effect of L-Glucose on necrosis of iPSC-CMs. Related to Figure 5, 6, 7 and 8.
iPSC-CMs were treated with L-glucose (25 mM) for 72 hours and subjected to SI/RO (simulated ischemia for 4 hours) and reoxygenation for 24 hours) injury under normal (NG) and high glucose (HG) conditions. n=6; *p<0.0001 vs NG & L-Glucose.
Statistics: One-way ANOVA. Data are represented as mean ± SEM.

B. miR-302a expression in iPSC-CMs after transfection with miR-302a mimic. Related to Figure 7 and 8. Time PCR quantitation of miR-302a in iPSC-CMs after 24 hours of transfection with miR-302a-mimic (20 nM) and 72 hours of normal (NG) and high glucose (HG) conditions. Sno-202 was used to normalize miRNA-302a expression. n=3; *p<0.0001 vs Control (NG & HG).
Statistics: One-way ANOVA. Data are represented as mean ± SEM.

Transparent Methods

Study Design

To elucidate the distinct signaling mechanisms involved in salutary effect of rapamycin (RAPA), we performed conscious myocardial ischemia/reperfusion (I/R) injury in preclinical diabetic rabbit and simulated ischemia/reoxygenation (SI/RO) injury in high-glucose (HG)-treated (human induced pluripotent stem cells-derived cardiomyocytes (hiPSC-CMs). Before induction of diabetes with alloxan, we ensured the similar average initial body weight and cardiac function in aged-matched rabbits. After alloxan treatment, body weight and glucose levels were monitored twice a day to confirm the induction of diabetes. Control and diabetic rabbits were randomized and subjected to conscious I/R injury with/without infusion of RAPA at the onset of reperfusion. After 72 hours of reperfusion, cardiac function was monitored. After sacrifice, myocardial infarct size, apoptosis, plasma troponin I, mTOR activity, expression of microRNAs (miRs) and PTEN were assessed. Typically, minimum four to six samples were used for *in vivo* experiments. The experimenters were blinded to group assignment and the outcome of the assessment. Data from six rabbits, which died within 14 days of alloxan treatment, were excluded from this study. Four rabbits were not included in I/R protocol because their blood glucose level were below 220 mg/dL. To examine the cause and effect relationship of miR-302a in regulating PTEN-AKT signaling, *in vitro* studies with three to six independent experiments were performed in HG-treated hiPSC-CMs with inhibition or overexpression of miR-302a followed by SI/RO.

Induction of diabetes in rabbit

New Zealand male rabbits (age: 3-4 months; body weight (BW): 2.8-3.0 kg; n=**90**) were purchased from Robinson Services Incorporated (RSI, NC, USA). All animal experiments were performed in accordance with USDA regulations and were approved by the Institutional Animal Care and Use Committee at the Virginia Commonwealth University. Diabetes in rabbits was induced as described by Wang *et al.*, 2010 (Wang et al., 2010) with modifications (**Figure 1A**). Briefly, alloxan monohydrate (125 mg/kg of BW, Sigma Aldrich, MO, USA) was administered via ear vein for 10 minutes in lightly sedated rabbits (**n=63**) with ketamine (35 mg/kg of BW), Xylazine (5 mg/kg of BW) and Atropine (5 mg/kg of BW). Blood glucose level was measured using Contour glucose meter (Bayer, NJ, USA) at 1, 2, 3 and 4 hours post-alloxan injection to prevent hypoglycemic shock. If blood sugar level dropped below 70 mg/dL, animals were supplemented with dextrose (10 ml of 10%, i.m.). Animals were provided with 20% glucose in drinking water for 3 days. Glucose levels were carefully monitored twice a day and animals were given insulin (1-2 U/kg of BW, Novalin-R, Nova Nordisk Pharmaceutical, NJ, USA) if glucose level exceeded 400-500 mg/dL. Body weights (BW) were also recorded weekly.

Conscious ischemia/reperfusion injury

After 4 weeks of alloxan treatment, animals with blood glucose consistently above 220 mg/dL were considered diabetic and included in the protocol for further experiments. Rabbits were randomized into five groups: Control (n=7), I/R (n=20), DM (n=10), DM with I/R (DM+I/R, n=23) and DM+I/R treated with RAPA (DM+I/R+RAPA, n=20). The rabbit model of conscious I/R has been described previously (Jones et al., 2015; Torrado et al., 2018). Briefly, after anesthetizing with sodium pentobarbital (35 mg/kg of BW; i.v.), the rabbit was intubated and connected to a ventilator (28-30 breaths/min). The heart was exposed through a left thoracotomy in the fourth intercostal space. After opening the pericardium, a 3-0 taper needled silk suture was passed beneath a major branch of the left coronary artery perpendicularly. A balloon occluder was placed on top of the coronary artery and secured with the 3-0 silk on the anterior LV wall and the chest wall was closed. Seven days after successful implantation of balloon occluder, the sedated rabbits were subjected to a 45-min conscious ischemia followed by 3 days of reperfusion by inflating/deflating the hydraulic balloon occluder. Ketoprofen (3.0 mg/kg, s.c.) was administered 2 h before and diazepam (4 mg/kg of BW; i.p.) was given 20 min before the onset of ischemia. Based on the treatment groups animals were infused with either RAPA (0.25 mg/kg of BW; i.v.) or DMSO (vehicle) 5 min before the onset of reperfusion via marginal ear vein catheter. Blood was collected in heparinized tube at baseline and at an interval of 1, 2, 4 and 24 hours after the initiation of reperfusion and centrifuged to separate plasma which was stored at -20^{o}C.

Assessment of Cardiac Function

Echocardiographic measurements were performed following a sedation protocol (inhaled isoflurane 2.5%) using a Vevo2100^{TM} (VisualSonics Inc., Toronto, Canada) at different time points, before (baseline) and after alloxan treatment, after implantation, and 3 days post I/R as per protocol to randomize the rabbits in DM, DM+I/R, DM+I/R+RAPA cohorts. Two operators, blinded to rabbit cohort allocation, performed repeated rounds of echocardiography to minimize inter- and intra-observer variations. Short and long parasternal views were obtained to measure cavity dimensions. The LVEF, left ventricular end-diastolic, end-systolic and stroke volumes were calculated by tracing the end- and epicardial boarder during contraction (Torrado et al., 2018). The obtained images were analyzed using Vevo LAB 3.2.0 software.

Measurement of hemodynamics

The animals were stabilized for at least 15 min and vital cardiac parameters including mean arterial pressure, systolic pressure, diastolic pressure and heart rate were monitored throughout the conscious I/R protocol via a transducer sensor probe secured to arterial line of rabbit ear connected to Blood Pressure Analyzer (BPA, Digi-Med, KY USA).

Infarct size measurement

After completion of I/R protocol, the rabbits were anesthetized with pentobarbital (50 mg/kg of BW; i.v.) and euthanized using potassium chloride via catheter connected to ear auricular artery. After excision, the heart was mounted on Langendorff apparatus and perfused with Krebs-Henseleit buffer. The coronary artery was tied and 5% solution of phthalo blue dye infused through the aortic root. The heart was cut into 5-6 transverse slices and stained with 1% triphenyltetrazolium chloride (TTC) and then fixed in 10% formalin and photographed (Torrado et al., 2018). The red region was marked as viable area, blue tissue as non-risk region and white area was considered as necrotic (**Figure 1C**). The infarct size was quantified using image J software (Bethesda, NIH, USA).

Evaluation of Apoptosis

The risk area of the LV was dissected, fixed in 10% formalin and 5µm thick sections were prepared after paraffin embedding. The sections were stained using a Terminal Deoxynucleotidyl Transferase dUTP Nick end Labeling (TUNEL) kit (BD Bioscience, San Jose, CA). The slides were then counter stained with troponin (mouse Troponin T antibody, Sigma-Aldrich, Missouri, USA) and anti-mouse IgG (H+L), F(ab')2 Fragment (Alexa Fluor® 594 Conjugate, Cell Signaling, MA, USA), and fixed with DAPI anti-fade mount solution. The apoptotic cells (green nuclei) and total cells (DAPI-blue nuclei) were counted under a fluorescence microscope, and the data was plotted as the percentage of apoptotic cells to total cells.

Cardiac Troponin I measurement

Cardiac troponin I (cTnI) was measured in the plasma samples using Ultra-Sensitive Rabbit Cardiac Troponin-I ELISA kit (Life Diagnostics Inc, USA) (Jones et al., 2015; Torrado et al., 2018). Each assay was performed in duplicate in a blinded fashion.

Simulated Ischemia/Reoxygenation (SI/RO) in hiPSC-CMs

iCell Cardiomyocytes, human cardiomyocytes derived from induced pluripotent stem cells (hiPSC-CM, Cellular Dynamics International, CDI INC. Madison, WI) were treated with Maintenance Medium containing 10 mM Galactose in addition to glucose (NG:5 mM) or high glucose (HG:25 mM) for 72 hours (Rana et al., 2012). Subsequently, the cells were subjected to SI for 4 hours in a tri-gas incubator by adjusting 1-2% O_2 and 5% CO_2 at 37°C with an "ischemia buffer" (Das et al., 2006; Das et al., 2005). The cells were reoxygenated (RO) under normoxic conditions for 24 hours by replacing the ischemic buffer with normal Maintenance medium in addition to NG or HG.

A subset of cells were treated with RAPA (100 nM) during RO under both NG and HG conditions. Cell death was assessed by Trypan blue exclusion assay and apoptosis by TUNEL staining (Das et al., 2006; Das et al., 2005).

Bioinformatic analysis of Rabbit miRNA

Based on the annotation data obtained from miRBASE (http://www.mirbase.org), 12 potential miRNAs were predicted to express in the rabbit species **(Table S2)**. We analyzed the expression profile of 9 microRNAs, which showed sequence similarity to human isoforms by real time PCR. Moreover, target prediction analysis using TargetScan (Garcia et al., 2011; Lewis et al., 2005) identified the potential binding site for miR-302a-3p on the 3'UTR of PTEN mRNA **(Figure S5)**. Published literature (Poliseno et al., 2010) also provided further evidence for miR-302a and PTEN interaction.

PTEN 3'UTR Luciferase Assay

The specificity of miR-302a binding to 3'-UTR of PTEN was confirmed by Dual luciferase reporter assay. The fragment of PTEN 3'-UTR (3001-3997) which includes the binding region of miR-302a was amplified from mouse genomic DNA and cloned into pmirGLO Dual-Luciferase miRNA target expression Vector (Promega Corp., WI, USA) using Sac1 and Xba1 restriction sites. H9C2 cells (ATCC, VA, USA) were transfected with pmiRGLO vector containing PTEN 3'UTR binding sequences for miR-302a or empty vector along with either miR-302a mimic (miR-302a-3p-5'uaagugcuuccauguuuugguga-3') or miR mimic negative control (Applied Biological Materials Inc., BC, Canada) using Lipofectamine 2000 (Invitrogen, NY, USA). The intensity of firefly luciferase corresponding to miR-302a activity was analyzed using Dual luciferase assay system (Promega Corp., WI, USA). Renilla luminescence served as internal control for transfection efficiency and normalization. The data was presented as percentage of Firefly to Renilla luciferase ratio normalized to empty vector control (**Figure S5B**). The following primers were used to amplify the PTEN-3'UTR from mouse genomic DNA: PTEN-Sac1-FP-5'-ACGAGCTCCCATCTCCTATGTAATC-3'and PTEN-Xba1-RP-5'-TCTCTAGAGAGTGAAACTGATGAGGTAT-3'.

LNA based miRNA-302a inhibition and miRNA-302a overexpression

LNA™-enhanced hsa-miR-302a-3p inhibitor **(**miRCURY-LNA-Power Inhibitor, 5'-fluorescein labeled; $^{5'}$-CACCAAAACATGGAAGCACTT-$^{3'}$/36-FAM/) was purchased from Exiqon Company (Woburn, MA, USA). miRCURY-LNA-miR-power inhibitor contains phosphorothioate bonds which enhances the transfection efficiency of iCell Cardiomyocyte. miCURY-LNA^{TM}-miR inhibitor control ($^{5'}$-TAACACGTCTATACGCCCA-$^{3'}$) was used as a negative control (scramble). miR-302a mimic (hsa-miR-302a-3p mimic) was purchased from Applied Biological Materials Inc (Richmond, BC, Canada).

Transfection of hiPSC-CMs

hiPSC-CM cells were transfected with hsa-miR 302a-3p inhibitor (20 nM) or miR-control inhibitor or miR-302a mimic (20 nM) using ViaFect^{TM} Transfection Reagent (Promega Corp. Madison, WI). After 48 hours, cells were subjected to high glucose (HG) conditions for 72 hours and SI/RO protocol.

Western blot analysis

Total soluble protein was extracted from the frozen LV tissues/hiPSC-CMs with lysis buffer (Cell Signaling, MA, USA). Protein samples (50 µg) were resolved by SDS-PAGE, transferred onto a nitrocellulose membrane. Membranes were incubated overnight with mouse monoclonal antibody specific for PTEN, p-AKT (S^{473}), p-AKT (Thr308), AKT, p-S6, S6, Bcl-2, Bax and GAPDH (Cell Signaling, MA, USA). The blots were then incubated for 1-hour with anti-mouse secondary horseradish peroxidase-conjugated antibody (GE healthcare, PA, USA) and developed using

Western Lightning Plus–ECL substrate (PerkinElmer, MA, USA). The densitometry analysis to quantitate the intensity of the protein band was performed using Image J software (NIH, Bethesda, MD).

Lipid Peroxidation Assay

Lipid peroxidation was measured by formation of malondialdehyde (MDA) in heart tissues using an assay kit (BioVision, CA, USA) according to the manufacturer's protocol (Das et al., 2014).

RNA isolation and miRNA expression

Total RNA was isolated from frozen LV tissue/hiPSC-CMs using miRNeasy mini kit (QIAGEN Sciences, MD, USA). Concentration and the purity of the isolated RNA was verified using Nanodrop ND-1000 spectrophotometer (Agilent technologies, CA, USA). Total RNA (10 ng) was subjected to reverse transcription reaction with miRNA-specific RT-primer using microRNA reverse transcription kit (Applied Biosystems, CA, USA). TaqMan™ miRNA assay probe (Occ-miR-302a-UAAGUGCUUCCAUGUUUUGGUGA) was performed (Applied Biosystems, CA, USA) to determine the expression level of miR-302a and normalized using U6 or Sno-202 small RNA. All other miRNAs (miR-191, miR-290, miR-294, miR-512a, miR-302b, c,d, miR-367) were quantified using TaqMan™miRNA Assay from Applied Biosystems. To quantify the mRNA of PTEN, total RNA (2 µg) were reverse transcribed using high capacity cDNA synthesis kit (Applied Biosystems). cDNA was subjected to real-time-PCR using TaqMan™ mRNA Assay for PTEN quantification and normalized with GAPDH using Roche Light cycler 480 II (Roche Applied Science, IN, USA).

Statistical Analysis

Statistical analysis was performed with GraphPad Prism 8 (GraphPad Software Inc. La Jolla, CA). The data are presented as mean±SE for each treatment group, along with unadjusted 2-tailed p values <0.05 were considered statistically significant. One-way ANOVA + Bonferroni post-hoc test was used for unpaired data to compare 2 and 3 groups, respectively. Two-way analysis of variance (ANOVA) with repeated measures + Bonferroni post hoc test were used to compare pre-intervention and post-intervention variables when appropriate.

Ethics Statement

All animal experiments were performed in accordance with USDA regulations and were approved by the Institutional Animal Care and Use Committee at the Virginia Commonwealth University.

Supplemental References

Das, A., Durrant, D., Koka, S., Salloum, F.N., Xi, L., and Kukreja, R.C. (2014). Mammalian target of rapamycin (mTOR) inhibition with rapamycin improves cardiac function in type 2 diabetic mice: potential role of attenuated oxidative stress and altered contractile protein expression. J Biol Chem *289*, 4145-4160.

Das, A., Smolenski, A., Lohmann, S.M., and Kukreja, R.C. (2006). Cyclic GMP-dependent protein kinase Ialpha attenuates necrosis and apoptosis following ischemia/reoxygenation in adult cardiomyocyte. J Biol Chem *281*, 38644-38652.

Das, A., Xi, L., and Kukreja, R.C. (2005). Phosphodiesterase-5 inhibitor sildenafil preconditions adult cardiac myocytes against necrosis and apoptosis. Essential role of nitric oxide signaling. J Biol Chem *280*, 12944-12955.

Garcia, D.M., Baek, D., Shin, C., Bell, G.W., Grimson, A., and Bartel, D.P. (2011). Weak seed-pairing stability and high target-site abundance decrease the proficiency of lsy-6 and other microRNAs. Nat Struct Mol Biol *18*, 1139-1146.

Jones, S.P., Tang, X.L., Guo, Y., Steenbergen, C., Lefer, D.J., Kukreja, R.C., Kong, M., Li, Q., Bhushan, S., Zhu, X.*, et al.* (2015). The NHLBI-sponsored Consortium for preclinicAl assESsment of cARdioprotective therapies (CAESAR): a new paradigm for rigorous, accurate, and reproducible evaluation of putative infarct-sparing interventions in mice, rabbits, and pigs. Circ Res *116*, 572-586.

Lewis, B.P., Burge, C.B., and Bartel, D.P. (2005). Conserved seed pairing, often flanked by adenosines, indicates that thousands of human genes are microRNA targets. Cell *120*, 15-20.

Poliseno, L., Salmena, L., Riccardi, L., Fornari, A., Song, M.S., Hobbs, R.M., Sportoletti, P., Varmeh, S., Egia, A., Fedele, G.*, et al.* (2010). Identification of the miR-106b~25 microRNA cluster as a proto-oncogenic PTEN-targeting intron that cooperates with its host gene MCM7 in transformation. Sci Signal *3*, ra29.

Rana, P., Anson, B., Engle, S., and Will, Y. (2012). Characterization of human-induced pluripotent stem cell-derived cardiomyocytes: bioenergetics and utilization in safety screening. Toxicol Sci *130*, 117-131.

Torrado, J., Cain, C., Mauro, A.G., Romeo, F., Ockaili, R., Chau, V.Q., Nestler, J.A., Devarakonda, T., Ghosh, S., Das, A.*, et al.* (2018). Sacubitril/Valsartan Averts Adverse Post-Infarction Ventricular Remodeling and Preserves Systolic Function in Rabbits. J Am Coll Cardiol *72*, 2342-2356.

Wang, J., Wan, R., Mo, Y., Zhang, Q., Sherwood, L.C., and Chien, S. (2010). Creating a long-term diabetic rabbit model. Exp Diabetes Res *2010*, 289614.